swelling and redness of the limb and later, ankylosis. The average of the macroscopic score was expressed as a cumulative value for all paws, with a maximum possible score of 16 per mouse. The in vivo experiments were performed with 10 mice per group and repeated twice to ensure reproducibility.

In vivo glycolipids treatment and antibody treatment. Synthetic glycolipids were used to treat CIA. Starting from the indicated day, mice were injected intraperitoneally twice per week with either OCH or α-GC at a dose of 500 μg/kg. The control mice were injected with vehicle alone (10% DMSO in phosphate buffered saline [PBS]). To neutralize IL-4 or IL-10, anti–IL-4 monoclonal antibody (mAb) (11B11) or anti–IL-10 mAb (JES-2A5) (500 μg per mouse) was injected intraperitoneally 2 hours before glycolipid administration.

Histopathologic study. Forepaws were removed from mice killed 50 days after the first immunization of CII, then fixed in buffered formalin, decalcified, embedded in paraffin, sectioned, and stained with hematoxylin and eosin for histopathologic analysis.

NKT cell preparation. NK1.1-positive T cells were purified from the liver of 6–8-week-old B6 mice. Liver mononuclear cells were prepared by Percoll density-gradient centrifugation. Prepared cells were then incubated with phycoerythrin-conjugated NK1.1 mAb and fluorescein isothiocyanate–conjugated CD3 mAb (BD PharMingen, San Jose, CA). The stained cells were sorted into $NK1.1^+$,$CD3^+$ cells. The purity of the sorted cells was >95%.

Quantitative reverse transcriptase–polymerase chain reaction (RT-PCR). Total RNA was extracted with an RNeasy kit (Qiagen KK, Tokyo, Japan) from purified $NK1.1^+$ T cells. Random hexamer-primed complementary DNA was prepared with the First-Strand cDNA Synthesis Kit (Invitrogen, Carlsbad, CA). For quantitative analysis of cytokines, we used the LightCycler quantitative PCR system (Roche Molecular Biochemicals, Mannheim, Germany) and performed quantitative PCR with a commercial kit (LightCycler-DNA Master SYBR Green I; Roche Molecular Biochemicals). The PCR amplification was repeated 40 times (for 15 seconds at 95°C, 5 seconds at 60°C, and 10 seconds at 72°C). All PCR reactions were normalized by GAPDH expression.

Enzyme-linked immunosorbent assay (ELISA). To detect CII-specific IgG1 and IgG2a, chicken CII or bovine CII (5 μg/ml) was coated onto ELISA plates (Sumitomo Bakelite, Tokyo, Japan) at 4°C overnight. After blocking with 3% bovine serum albumin in PBS, serially diluted serum samples were added onto CII-coated wells. The plates were incubated with biotin-labeled anti-IgG1 and anti-IgG2a (Southern Biotechnology, Birmingham, AL) or anti-IgG antibody (CN/Cappel, Aurora, OH) for 1 hour and then incubated with streptavidin–peroxidase. After addition of substrate, the reaction was evaluated. The levels of IL-4, IL-10, and IFNγ in serum were measured by standard sandwich ELISA, using purified and biotinylated mAb pairs and standards (BD PharMingen).

RESULTS

Suppression of CIA development by OCH. In order to determine whether stimulation of NKT cells modulates arthritis, we first examined the effect of α-GC, a prototypic ligand for NKT cells, on the development of CIA. Early studies showed that CIA is restricted to mouse strains bearing the $H\text{-}2^q$, $H\text{-}2^r$, or $H\text{-}2^s$ haplotype (29) and is generally induced in DBA/1 mice. More recently, modified immunization conditions that are sufficient to induce CIA in B6 mice have been developed; this allowed us to study CIA in knockout mice with a B6 background, which eliminated the need to backcross the knockout mice onto a DBA/1 background (30,31). The histologic and immunologic characteristics of the disease induced in B6 mice have been shown to be similar to those in DBA/1 mice, even though B6 mice have a slightly delayed onset and less uniformly severe disease (31). We immunized B6 mice with chicken CII in CFA to elicit CIA as described previously (30) and then injected mice intraperitoneally with either α-GC or vehicle alone twice per week starting from the day of the second immunization. As shown in Figure 1B, α-GC treatment did not improve the arthritis score significantly. We next examined the effect of OCH on CIA. The mean maximum clinical CIA score was profoundly reduced in OCH-treated B6 mice (Figure 1B and Table 1). The incidence and the time of onset of disease were not significantly different between the OCH-treated group and the control group.

Table 1. Clinical scores of collagen-induced arthritis in C57BL/6 and J_α281-knockout mice*

Mice, treatment	Incidence, %	Maximum score, mean ± SEM	Days to onset, mean ± SEM
C57BL/6 (wild-type)			
Vehicle	100	13.0 ± 0.83	23.8 ± 0.48
α-GC	100	9.8 ± 2.37	24.2 ± 0.48
OCH	100	4.6 ± 0.92†	24.2 ± 0.48
J_α281-knockout			
Vehicle	100	5.5 ± 0.5	24 ± 0.58
OCH	100	5.75 ± 0.25	23.5 ± 0.5

* C57BL/6 mice or J_α281-knockout mice were sensitized with chicken type II collagen for induction of arthritis.
Vehicle or 500 μg/kg of α-galactosylceramide (α-GC) or OCH was injected intraperitoneally twice per week from day 21. Data are from 5 mice per group.
† $P < 0.05$ versus control vehicle, by Mann-Whitney U test.

To investigate the role of V_α14 NKT cells in the suppression of CIA by OCH, we examined the ability of OCH to modulate disease in J_α281-knockout mice, in which V_α14 NKT cells are absent (32). Administration of OCH did not modulate the clinical course of CIA in J_α281-knockout mice compared with mice treated with vehicle alone (Figure 1C and Table 1). These results indicate that OCH-mediated suppression of CIA requires NKT cells.

In addition to visual scoring, on day 50 after

disease induction we analyzed the histologic features in the joints of forepaws of wild-type B6 mice treated with OCH or α-GC. As shown in Figure 2, in the control and α-GC–treated groups there was severe arthritis in the joints, associated with massive cell infiltration, cartilage erosion, and bone destruction. These histologic features were significantly less apparent in the group of mice treated with OCH. These results demonstrated that administration of OCH ameliorated CIA, whereas α-GC had little effect on CIA in B6 mice.

Selective induction by OCH of NKT cell–mediated IL-4 and IL-10 production. Activation of NKT cells leads to the rapid production of a variety of cytokines, including IL-4, which promotes Th2 differentiation, and IFNγ, which promotes Th1 differentiation. Previously we demonstrated that OCH stimulates NKT cells to produce predominantly IL-4, whereas α-GC stimulates NKT cells to produce both IL-4 and IFNγ (27). IL-10, as well as IL-4, has also been reported to suppress CIA (1) and to be involved in α-GC–mediated inhibition of diabetes in the NOD mouse (33). These data led us to examine whether IL-10 was induced by OCH stimulation. We measured serum levels of IL-10 in addition to IL-4 and IFNγ, 2 hours and 12 hours after intraperitoneal injection of either OCH or α-GC into B6 mice. As shown in Figure 3A, OCH, as well as α-GC, caused an elevation in IL-10 levels. Consistent with previous results, OCH injection induced a rapid rise in IL-4 levels along with a much less marked increase in levels of IFNγ. Injection of α-GC induced the production of IL-4 and IFNγ (Figure 3A). NKT cell–deficient $J_{\alpha}281$-knockout mice did not exhibit a response to either α-GC or OCH (Figure 3A), indicating that the increase in cytokine levels in B6 mice was mediated by NKT cells.

To further clarify the difference in gene expression by NKT cells stimulated with OCH or α-GC, we performed quantitative RT-PCR to detect the levels of expression of major contributors to joint destruction, such as TNFα and receptor activator of NF-κB ligand (RANKL) in stimulated NKT cells in vivo. We sorted $NK1.1^+$ T cells from liver mononuclear cells of B6 mice 1.5 hours after administration of either OCH or α-GC. As shown in Figure 3B, α-GC stimulation induced expression of TNFα and RANKL genes. In contrast, OCH stimulation induced much lower levels of TNFα and RANKL expression.

Efficient inhibition by OCH of CIA development in SJL mice. In a screen of laboratory mouse strains, NKT cells in SJL mice, which exhibit a marked propensity to the Th1-mediated autoimmune diseases, were

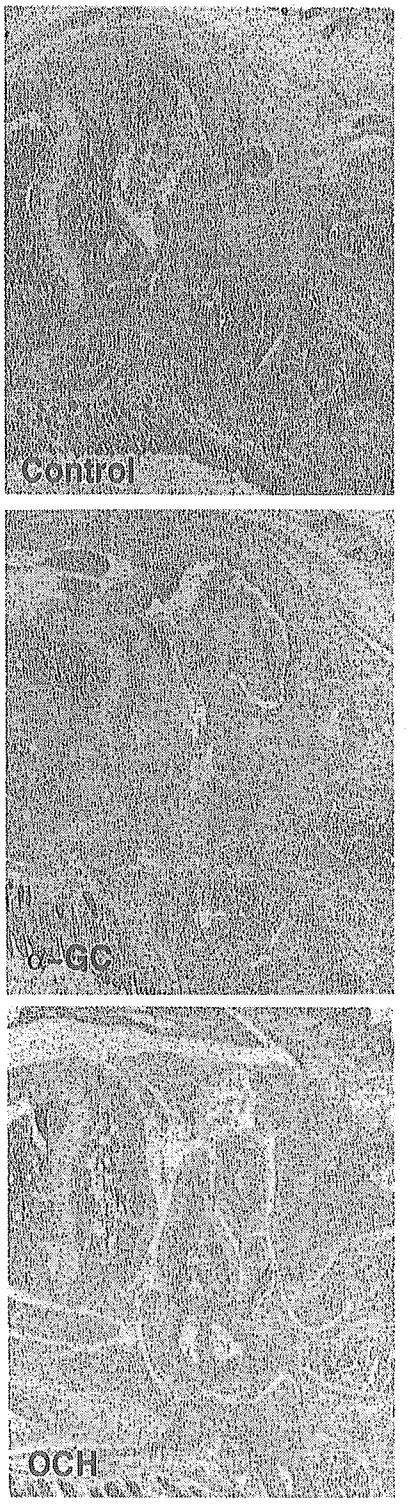

Figure 2. Histopathologic assessment of arthritic wrist joints of mice treated with control vehicle, α-galactosylceramide (α-GC), or OCH (hematoxylin and eosin stained; original magnification × 20).

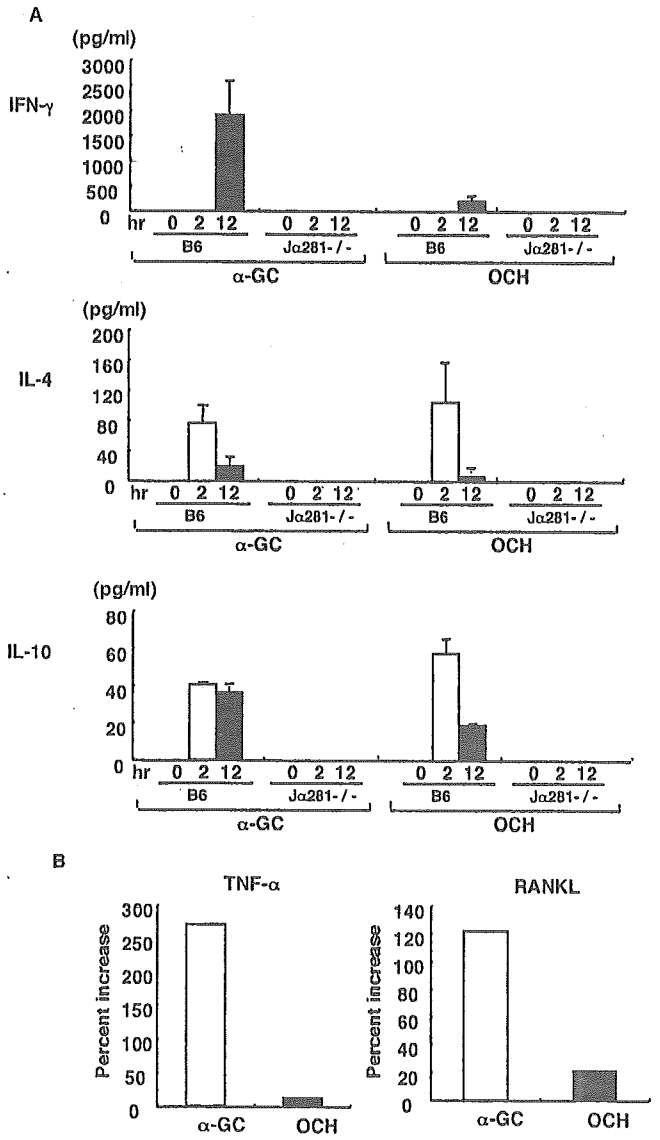

Figure 3. A, Change in serum cytokine levels after injection of OCH or α-GC in wild-type B6 and $J_{\alpha}281$-knockout mice. Serum levels of interferon-γ (IFNγ), interleukin-4 (IL-4), and IL-10 in B6 mice or $J_{\alpha}281$-knockout mice 2 hours (open bars) and 12 hours (solid bars) after intraperitoneal injection of OCH or α-GC were measured by enzyme-linked immunosorbent assay. **B,** Quantitative analysis of levels of tumor necrosis factor α (TNFα) and receptor activator of NF-κB ligand (RANKL) by reverse transcriptase–polymerase chain reaction. Total RNA was isolated from $NK1.1^+$ T cells of OCH- or α-GC–treated mice, and the percent increase was calculated based on the expression of each gene obtained in cells of vehicle-treated mice. Values are the mean and SEM (4 mice per group). See Figure 1 for other definitions.

found to be reduced in number and to have a profound defect in IL-4 secretion (19–23). Furthermore, recent studies of human autoimmune diseases demonstrated that patients with these diseases exhibited a decreased frequency of NKT cells in the periphery (15–18). These data led us to investigate whether OCH could ameliorate CIA in the autoimmune-prone mice with reduced numbers of and functional defects in NKT cells. Administration of OCH in SJL mice resulted in a rapid appearance of IL-4 and IL-10, although the levels of these cytokines were lower than those in B6 mice (data not shown). In contrast, IFNγ was barely detectable in the serum of SJL mice treated with OCH (data not shown), indicating that the cytokine profile induced by OCH stimulation was similar to that seen in B6 mice.

Next, we immunized SJL mice with bovine CII to induce CIA and then treated the mice with either OCH, α-GC, or vehicle alone. As shown in Figure 4A and Table 2, OCH administration efficiently inhibited the clinical course of CIA, whereas α-GC treatment had little effect on CIA in SJL mice. To examine the

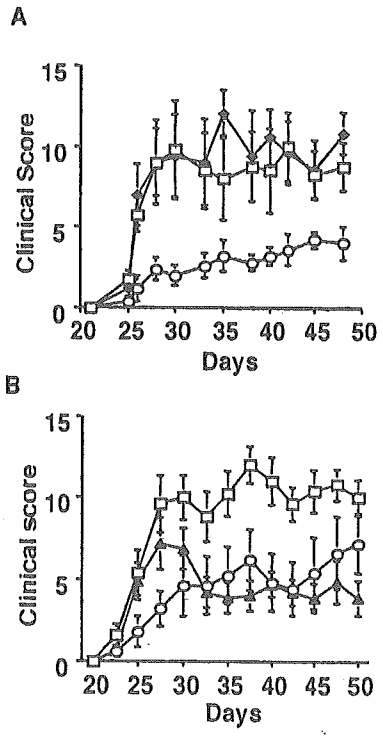

Figure 4. Effect of OCH on CIA in SJL mice. A, Clinical score of CIA in mice treated with 500 μg/kg of α-GC (◆), OCH (○), or vehicle (□) twice per week starting from day 21. **B,** Clinical score of CIA in mice treated with 500 μg/kg of vehicle starting from day 21 (□) or with OCH twice per week starting from day 21(○) or day 28 (▲). Data shown are from a single experiment representative of 2 identical experiments; values are the mean ± SEM (6 mice per group). See Figure 1 for definitions.

Table 2. Clinical scores of collagen-induced arthritis in SJL mice*

Time of injection, treatment	Incidence, %	Maximum score, mean ± SEM	Days to onset, mean ± SEM
Day 21 after immunization			
Vehicle	100	11.0 ± 2.35	24.0 ± 0.00
α-GC	100	12.4 ± 1.50	24.4 ± 0.40
OCH	100	5.2 ± 0.58†	28.8 ± 2.42
Day 21 or 28 after immunization			
Vehicle, day 21	100	12.6 ± 1.03	23.4 ± 0.40
OCH, day 21	100	7.0 ± 2.17†	26.8 ± 2.84
OCH, day 28	100	7.8 ± 1.35†	24.0 ± 0.45

* Mice were sensitized with chicken type II collagen for induction of arthritis. Vehicle or 500 μg/kg of α-galactosylceramide (α-GC) or OCH was injected intraperitoneally twice per week. Data are from 6 mice per group.
† $P < 0.05$ versus control vehicle, by Mann-Whitney U test.

potential therapeutic effect of OCH on established CIA, we injected OCH beginning on day 28 after the first immunization, when arthritis had already developed (Figure 4B and Table 2). The severity of arthritis gradually decreased after OCH treatment, and the disease was efficiently suppressed within 1 week. These results suggest that OCH has a therapeutic effect on established CIA in autoimmune-prone mice.

Promotion of CII-specific Th2 responses by OCH. OCH has been demonstrated to alter the cytokine profile of autoantigen-specific T cells in vivo (27). We therefore speculated that the OCH-mediated inhibition of arthritis might be due to a modulation of the Th1/Th2 balance, resulting from a Th2 bias of CII-reactive T cells. To explore this possibility, we measured CII-specific immunoglobulin isotype levels 50 days after induction of CIA. It is generally accepted that elevation of antigen-specific IgG2a antibody results from augmentation of a Th1 immune response to the antigen, whereas a higher level of IgG1 antibody would reflect a stronger Th2 response to the antigen. In OCH-treated mice there was a greater reduction in the level of IgG2a antibody specific to CII versus IgG1 specific to CII (Figure 5A). Consequently, the IgG1:IgG2a ratio was elevated in mice treated with OCH (Figure 5B), indicating that the suppression of CIA by OCH is associated with a Th2 bias of CII-reactive T cells.

Critical role of IL-4 and IL-10 in OCH-mediated suppression of CIA. To confirm the involvement of IL-4 and IL-10 in the suppression of CIA, we next examined whether the inhibitory effect of OCH was abrogated after neutralization of IL-4 or IL-10 in vivo. Groups of SJL mice were injected with anti–IL-4 or anti–IL-10 mAb 2 hours before OCH or vehicle was administered. OCH-mediated suppression of CIA was partially abolished when anti–IL-4 mAb was injected (Table 3). More remarkably, in the presence of anti–IL-10 mAb, the protective effect of OCH against CIA was no longer evident at all (Table 3). Injection of neutralizing antibody to either IL-10 or IL-4 reversed the beneficial effect of administration of OCH in B6 mice also (data not shown). These results imply that IL-4 and IL-10 are critical in the OCH-mediated suppression of CIA and are consistent with our hypothesis that OCH modulates CIA by stimulating production of Th2 cytokines by NKT cells.

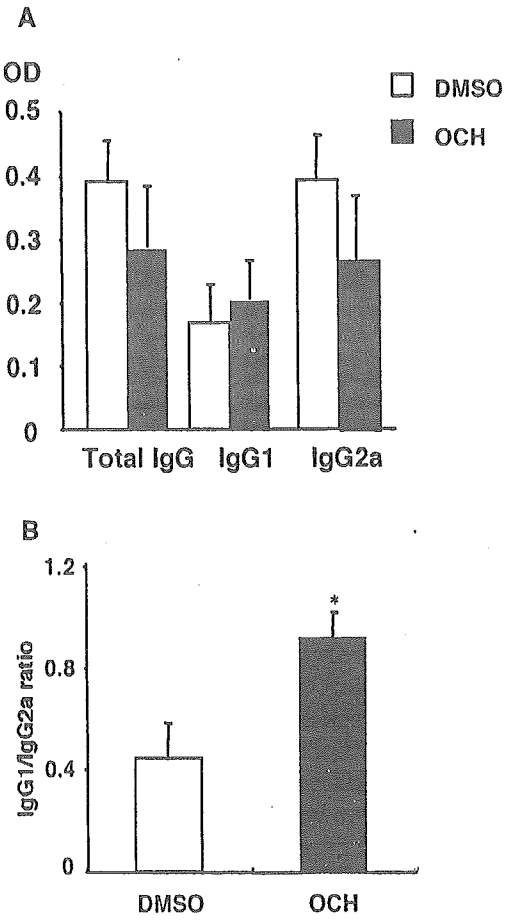

Figure 5. Effect of OCH on type II collagen (CII)–specific responses. Individual serum samples obtained on day 50 after induction of arthritis were analyzed as indicated in Materials and Methods. **A**, CII-specific antibody responses in OCH- or control vehicle (DMSO)–treated mice. **B**, IgG1:IgG2a ratio in OCH- or vehicle-treated mice. Values are the mean and SEM (n = 5). * = $P < 0.05$ versus control, by Mann-Whitney U test. OD = optical density.

Table 3. Abrogation of the ability of OCH to suppress collagen-induced arthritis after neutralization of IL-10 or IL-4 in vivo*

Treatment	Incidence, %	Maximum score, mean ± SEM	Days to onset, mean ± SEM
Control IgG			
Vehicle	100	12.8 ± 1.85	28.4 ± 0.60
OCH	90	5.0 ± 2.00†	29.0 ± 0.00
Anti–IL-10 mAb			
Vehicle	100	10.5 ± 1.86	29.0 ± 0.00
OCH	100	11.4 ± 1.44	28.4 ± 0.60
Anti–IL-4 mAb			
Vehicle	100	9.75 ± 2.84	27.5 ± 0.87
OCH	100	7.0 ± 0.45	27.8 ± 0.73

* SJL mice were sensitized with bovine type II collagen for induction of arthritis. Vehicle or 500 μg/kg of OCH was injected intraperitoneally twice per week from day 21. Anti–interleukin-10 (anti–IL-10) or anti–IL-4 monoclonal antibody (mAb) (500 μg per mouse) was injected each time vehicle or OCH was administered. Data are from 5 mice per group.
† $P < 0.05$ versus control vehicle, by Mann-Whitney U test.

DISCUSSION

A number of studies have shown that treatment with Th2-promoting cytokines or with monoclonal antibodies directed against Th1-promoting cytokines can effectively protect against the development of CIA in mice (1–11). Here we have demonstrated that specific activation of NKT cells with their ligand OCH provides an alternative way to shift the balance from a pathogenic Th1 response toward a protective Th2 response and that disease protection is dependent on NKT cells.

We also identified a critical role of the Th2 cytokines IL-4 and IL-10 in the ability of OCH to confer protection against CIA. Recently, local delivery of Th2 cytokines, using hybridomas (8) or dendritic cells (10,11) transfected with either IL-4 or IL-10, was found to be effective in the prevention of arthritis in animal models. In light of the fact that NKT cells are known to rapidly invade and accumulate in inflammatory lesions in a manner similar to inflammatory cells (34), stimulation of NKT cells to selectively induce Th2 cytokines might be a powerful strategy to deliver these cytokines to inflammatory lesions. It has been shown in vivo that neutralizing of IL-10, but not IL-4, increases the severity of CIA in DBA mice (3). However, we did not observe worsening of the clinical course of arthritis by neutralizing IL-4 or IL-10 in SJL mice in this study. Also in B6 mice, the clinical course of arthritis was not worsened when we neutralized IL-4 or IL-10 using the same mAb. Although the precise reason for the discrepancy with results of the earlier study is not clear, it may be because IL-4 and IL-10 levels were not high enough to modulate the severity of the disease in the natural course of arthritis in these strains.

The maximum score of CIA in the $J_\alpha 281$-knockout mouse was relatively low compared with that observed in wild-type B6 mice, suggesting that NKT cells may act as a modifier of the inflammation in the natural course of arthritis. We also observed a lower maximum score of CIA in CD1d-knockout mice (data not shown). Although the CD1d-knockout mice were backcrossed to B6 mice for only 6 generations, this observation further supports the notion that NKT cells increase the inflammation in the natural course of CIA. In contrast, the NOD and SJL strains of mice, which exhibit a marked propensity to the Th1-mediated autoimmune diseases, were found to have reduced numbers of NKT cells. Increasing the number of NKT cells in NOD mice by either transfer or transgenic expression of the invariant TCR V_α chain ($V_\alpha 14$–$J_\alpha 281$) resulted in a decrease in insulitis and diabetes, suggesting that NKT cells play a protective role in the development of diabetes (35,36). In these strains of mice, the defect of NKT cells may contribute to disease susceptibility. Identification of a natural antigen for NKT cells would provide further insight into the precise role of NKT cells in the pathogenesis of autoimmune diseases such as arthritis.

Alpha-galactosylceramide, a prototypic ligand for NKT cells, has been reported to prevent diabetes in NOD mice (22,33,37). Even though we confirmed that α-GC inhibited the development of diabetes in NOD mice (data not shown), we did not observe any inhibitory effect of α-GC on CIA. In a previous study, we demonstrated the inhibitory effect of α-GC on EAE induced in IFNγ-knockout mice but not in wild-type B6 mice (28), suggesting that α-GC is not effective in B6 mice because NKT cell–derived IFNγ would mask the therapeutic effect of the IL-4 simultaneously produced by NKT cells. In fact, the serum levels of IL-4 and IL-10 after administration of OCH or α-GC were similar, whereas IFNγ production was much lower after injection of OCH compared with α-GC injection. This suggests that the balance of Th1/Th2 cytokines produced by NKT cells is important with regard to the protection against Th1-mediated disease conferred by the glycolipid ligand. Thus, OCH is a unique ligand that is beneficial in the treatment of a wide variety of Th1-mediated autoimmune diseases.

Another advantage of using OCH rather than α-GC is the reduced production of factors that are harmful in arthritis, such as TNFα and RANKL. TNFα is one of the major contributors to joint inflammation and destruction (38). It induces the production of other

proinflammatory cytokines, stimulates endothelial cells to express adhesion molecules, increases the synthesis of metalloproteinases, and inhibits the synthesis of proteoglycans in cartilage (39). TNF levels are chronically elevated in the blood and, more specifically, in the joints, of patients with RA (40), and it has been proven that the blocking of TNF-related pathways is a strong therapeutic tool in RA (41). RANKL has emerged as one of the essential pathogenic factors in the destruction of cartilage and bone in RA (42–45). RANKL is part of the TNF ligand family and is an important regulator of both osteoclastogenesis and functions of the immune system, including lymph node organogenesis and lymphocyte development. Even though the roles of RANKL in the pathogenesis of RA during the chronic stage have not yet been elucidated, it is known that it is expressed both by synovial fibroblasts and by activated T lymphocytes derived from synovial tissue from patients with RA (43–45). Moreover, blocking of the RANKL pathway at the onset of adjuvant-induced arthritis prevents bone and cartilage destruction (42). Therefore, it is a noteworthy finding that OCH stimulation induces much lower levels of gene expression of TNFα and RANKL compared with stimulation by other glycolipid antigens such as α-GC.

We demonstrated in this study that OCH was effective in the treatment of established CIA in autoimmune-prone mice of the SJL strain, which have a quantitative and functional NKT cell deficiency; this suggests that OCH might be useful for the treatment of patients with various autoimmune diseases associated with reduced numbers of NKT cells. Furthermore, in contrast to classic MHC molecules, CD1d molecules are nonpolymorphic and are remarkably well conserved among the population and may become extremely valuable in the development of HLA-independent treatment approaches for autoimmune conditions. These findings highlight the potential use of OCH for therapeutic intervention in autoimmune diseases such as RA.

ACKNOWLEDGMENTS

We thank Masaru Taniguchi (Chiba University, Graduate School of Medicine, Chiba, Japan) for providing $J_{\alpha}281$-knockout mice, and Karen Mullane-Robinson (Boston, MA) for critical reading of the manuscript.

REFERENCES

1. Van Roon JAG, Lafeber FPJG, Bijlsma JWJ. Synergistic activity of interleukin-4 and interleukin-10 in suppression of inflammation and joint destruction in rheumatoid arthritis. Arthritis Rheum 2001;44:3–12.
2. Walmsley M, Katsikis PD, Abney E, Parry S, Williams RO, Maini RN, et al. Interleukin-10 inhibition of the progression of established collagen-induced arthritis. Arthritis Rheum 1996;39: 495–503.
3. Joosten LAB, Lubberts E, Durez P, Helsen MMA, Jacobs MJM, Goldman M, et al. Role of interleukin-4 and interleukin-10 in murine collagen-induced arthritis: protective effect of interleukin-4 and interleukin-10 treatment on cartilage destruction. Arthritis Rheum 1997;40:249–60.
4. Horsfall AC, Butler DM, Marinova L, Warden PJ, Williams RO, Maini RN, et al. Suppression of collagen-induced arthritis by continuous administration of IL-4. J Immunol 1997;159:5687–96.
5. Apparailly F, Verwaerde C, Jacquet C, Auriault C, Sany J, Jorgensen C. Adenovirus-mediated transfer of viral IL-10 gene inhibits murine collagen-induced arthritis. J Immunol 1998;160: 5213–20.
6. Ma Y, Thornton S, Duwel LE, Boivin GP, Giannini EH, Leiden JM, et al. Inhibition of collagen-induced arthritis in mice by viral IL-10 gene transfer. J Immunol 1998;161:1516–24.
7. Lubberts E, Joosten LAB, van den Bersselaar L, Helsen MMA, Bakker AC, van Meurs JBJ, et al. Adenoviral vector-mediated overexpression of IL-4 in the knee joint of mice with collagen-induced arthritis prevents cartilage destruction. J Immunol 1999; 163:4546–56.
8. Setoguchi K, Misaki Y, Araki Y, Fujio K, Kawahata K, Kitamura T, et al. Antigen-specific T cells transduced with IL-10 ameliorate experimentally induced arthritis without impairing the systemic immune response to the antigen. J Immunol 2000;165:5980–6.
9. Lubberts E, Joosten LAB, Chabaud M, van den Bersselaar L, Oppers B, Coenen-de Roo CJJ, et al. IL-4 gene therapy for collagen arthritis suppresses synovial IL-17 and osteoprotegerin ligand and prevents bone erosion. J Clin Invest 2000;105:1697–710.
10. Kim SH, Kim S, Evans CH, Ghivizzani SC, Oligino T, Robbins PD. Effective treatment of established murine collagen-induced arthritis by systemic administration of dendritic cells genetically modified to express IL-4. J Immunol 2001;166:3499–505.
11. Morita Y, Yang J, Gupta R, Shimizu K, Shelden EA, Endres J, et al. Dendritic cells genetically engineered to express IL-4 inhibit murine collagen-induced arthritis. J Clin Invest 2001;107:1275–84.
12. Bendelac A, Rivera MN, Park SH, Roark JH. Mouse CD1-specific NK1 T cells: development, specificity, and function. Annu Rev Immunol 1997;15:535–62.
13. Hong S, Scherer DC, Singh N, Mendiratta SK, Serizawa I, Koezuka Y, et al. Lipid antigen presentation in the immune system: lessons learned from CD1d knockout mice. Immunol Rev 1999;169:31–44.
14. Godfrey DI, Hammond KJ, Poulton LD, Smyth MJ, Baxter AG. NKT cells: facts, functions and fallacies. Immunol Today 2000;21: 573–83.
15. Sumida T, Sakamoto A, Murata H, Makino Y, Takahashi H, Yoshida S, et al. Selective reduction of T cells bearing invariant Vα24JαQ antigen receptor in patients with systemic sclerosis. J Exp Med 1995;182:1163–8.
16. Wilson SB, Kent SC, Patton KT, Orban T, Jackson RA, Exley M, et al. Extreme Th1 bias of invariant Vα24JαQ T cells in type 1 diabetes. Nature 1998;391:177–81.
17. Illes Z, Kondo T, Newcombe J, Oka N, Tabira T, Yamamura T. Differential expression of NK T cell Vα24JαQ invariant TCR chain in the lesions of multiple sclerosis and chronic inflammatory demyelinating polyneuropathy. J Immunol 2000;164:4375–81.
18. Kojo S, Adachi Y, Keino H, Taniguchi M, Sumida T. Dysfunction of T cell receptor AV24AJ18+,BV11+ double-negative regulatory natural killer T cells in autoimmune diseases. Arthritis Rheum 2001;44:1127–38.
19. Yoshimoto T, Bendelac A, Hu-Li J, Paul WE. Defective IgE

production by SJL mice is linked to the absence of CD4+, NK1.1+ T cells that promptly produce interleukin 4. Proc Natl Acad Sci U S A 1995;92:11931–4.
20. Mieza MA, Itoh T, Cui JQ, Makino Y, Kawano T, Tsuchida K, et al. Selective reduction of Vα14+ NK T cells associated with disease development in autoimmune-prone mice. J Immunol 1996;156:4035–40.
21. Gombert JM, Herbelin A, Tancrede-Bohin E, Dy M, Carnaud C, Bach J-F. Early quantitative and functional deficiency of NK1$^+$-like thymocytes in the NOD mouse. Eur J Immunol 1996;26: 2989–98.
22. Hong SH, Wilson MT, Serizawa I, Wu L, Singh N, Naidenko OV, et al. The natural killer T-cell ligand α-galactosylceramide prevents autoimmune diabetes in non-obese diabetic mice. Nat Med 2001;7:1052–6.
23. Singh AK, Wilson MT, Hong S, Olivares-Villagomez D, Du C, Stanic AK, et al. Natural killer T cell activation protects mice against experimental autoimmune encephalomyelitis. J Exp Med 2001;194:1801–11.
24. Kawano T, Cui J, Koezuka Y, Toura I, Kaneko Y, Motoki K, et al. CD1d-restricted and TCR-mediated activation of Vα14. Nature 1998;391:177–81.
25. Brossay L, Chioda M, Burdin N, Koezuka Y, Casorati G, Dellabona P, et al. CD1d-mediated recognition of an α-galactosylceramide by natural killer T cells is highly conserved through mammalian evolution. J Exp Med 1998;188:1521–8.
26. Spada FM, Koezuka Y Porcelli SA. CD1d-restricted recognition of syntheic glycolipid antigens by human natural killer T cells. J Exp Med 1998;188:1529–34.
27. Miyamoto K, Miyake S, Yamamura T. A synthetic glycolipid prevents autoimmune encephalomyelitis by inducing Th2 bias of natural killer T cells. Nature 2001;413:531–4.
28. Pal EA, Tabira T, Kawano T, Taniguchi M, Miyake S, Yamamura T. Costimulation-dependent modulation of experimental autoimmune encephalomyelitis by ligand stimulation of Vα14+ NK T cells. J Immunol 2001;166:662–8.
29. Courtenay JS, Dallman MJ, Dayan AD, Martin A, Mosedale B. Immunization against heterologous type II collagen induces arthritis in mice. Nature 1980;283:666–8.
30. Campbell IK, Rich MJ, Bischof RJ, Dunn AR, Grail D, Hamilton JA. Protection from collagen-induced arthritis in granulocyte-macrophage colony-stimulating factor-deficient mice. J Immunol 1998;161:3639–44.
31. Campbell IK, Hamilton JA, Wicks IP. Collagen-induced arthritis in C57BL/6 (H-2^b) mice: new insights into an important disease model of rheumatoid arthritis. Eur J Immunol 2000;30:1568–75.
32. Cui J, Shin T, Kawano T, Sato H, Kondo E, Toura I, et al. Requirement for Vα14 NKT cells in IL-12-mediated rejection of tumors. Science 1997;278:1623–6.
33. Sharif S, Arreaza GA, Zucker P, Mi Q-S, Sondhi J, Naidenko OV, et al. Activation of natural killer T cells by α-galactosylceramide treatment prevents the onset and recurrence of autoimmune type 1 diabetes. Nat Med 2001;7:1057–62.
34. Mempel M, Ronet C, Suarez F, Gilleron M, Puzo,G, van Kaer L, et al. Natural killer T cells restricted by the monomorphic MHC class 1b CD1d1 molecules behave like inflammatory cells. J Immunol 2002;168:365–71.
35. Hammond KJL, Poulton LD, Palmisano LJ, Silveria PA, Godfrey DJ, Bazter AG. α/β-T cell receptor (TCR)+CD4-CD8-(NKT) thymocytes prevent insulin-dependent diabetes mellitus in nonobese diabetic (NOD)/Lt mice by the influence of interleukin (IL)-4 and/or IL-10. J Exp Med 1998;187:1047–56.
36. Lehuen A, Lantz O, Beaudoin L, Laloux V, Carnaud C, Bendelac A, et al. Overexpression of natural killer T cells protects Vα14-Jα281 transgenic nonobese diabetic mice against diabetes. J Exp Med 1998;188:1831–9.
37. Wang B, Geng YB, Wang CR. CD1-restricted NK T cells protect nonobese diabetic mice from developing diabetes. J Exp Med 2001;194:313–9.
38. Keffer J, Probert L, Cazlaris H, Georgopoulos S, Kaslaris E, Kioussis D, et al. Transgenic mice expressing human tumor necrosis factor: a predictive genetic model of arthritis. EMBO J 1991;10:4025–31.
39. Choy EH, Panayi GS. Cytokine pathways and joint inflammation in rheumatoid arthritis. N Engl J Med 2001;344:907–16.
40. Brennan FM, Maini RN, Feldmann M. TNF alpha: a pivotal role in rheumatoid arthritis? Br J Rheumatol 1992;31:293–8.
41. Criscione LG, St Clair EW. Tumor necrosis factor-α antagonists for the treatment of rheumatic diseases. Curr Opin Rheumatol 2002;14:204–11.
42. Kong Y-Y, Feige U, Sarosi I, Bolon B, Tafuri A, Morony S, et al. Activated T cells regulate bone loss and joint destruction in adjuvant arthritis through osteoprotegerin ligand. Nature 1999; 402:304–9.
43. Gravallese EM, Manning C, Tsay A, Naito A, Pan C, Amento E, et al. Synovial tissue in rheumatoid arthritis is a source of osteoclast differentiation factor. Arthritis Rheum 2000;43:250–8.
44. Shigeyama Y, Pap T, Kunzler P, Simmen BR, Gay R, Gay S. Expression of osteoclast differentiation factor in rheumatoid arthritis. Arthritis Rheum 2000;43:2523–30.
45. Takayanagi H, Iizuka H, Juji T, Nakagawa T, Yamamoto A, Miyazaki T, et al. Involvement of receptor activator of nuclear factor κB ligand/osteoclast differentiation factor in osteoclastogenesis from synoviocytes in rheumatoid arthritis. Arthritis Rheum 2000;43:259–69.

International Immunology, Vol. 16, No. 2, pp. 223–230
doi: 10.1093/intimm/dxh018

Accumulation of $V_\alpha 7.2$–$J_\alpha 33$ invariant T cells in human autoimmune inflammatory lesions in the nervous system

Zsolt Illés[1], Michio Shimamura[2], Jia Newcombe[3], Nobuyuki Oka[4] and Takashi Yamamura[1]

[1]Department of Immunology, National Institute of Neuroscience, National Center of Neurology and Psychiatry, 4-1-1 Ogawahigashi, Kodaira, Tokyo 187-8502, Japan
[2]Laboratory of Developmental Immunology, Mitsubishi Kagaku Institute of Life Sciences, Tokyo 194-8511, Japan
[3]NeuroResource, Institute of Neurology, London WC1N 1PJ, UK
[4]Department of Neurology, Faculty of Medicine, Kyoto University, Kyoto 606-8507, Japan

Keywords: chronic inflammatory demyelinating polyneuropathy, invariant $V_\alpha 7.2$–$J_\alpha 33$ T cell, multiple sclerosis, NKT cell, single-strand conformation polymorphism

Abstract

T cells expressing an invariant TCR α chain and NK cell markers are expected to exhibit unique functions. Whereas much attention has been paid to CD1d-restricted NKT cells, a second NKT cell population bearing an invariant AV19–AJ33 TCR has recently been identified in mice and humans. Selection and/or expansion of this population require B cells, and would involve a non-classical class I-related molecule MR1. Although their preferential distribution in the gut mucosa indicates their role in the host response at the site of pathogen entry, it remains unknown whether they play an alternative role at different sites or in immunological disorders. Using single-strand conformation polymorphism clonotype analysis, we investigated the presence of the human AV19–AJ33 T cells ($V_\alpha 7.2$–$J_\alpha 33$ T cells) in autopsy samples from multiple sclerosis (MS) patients as well as in nerve biopsy samples from chronic inflammatory demyelinating polyneuropathy (CIDP) patients. Here we report that the $V_\alpha 7.2$–$J_\alpha 33$ T cells are accumulated in some of the central nervous system lesions of MS and in the majority of the peripheral nerve samples from CIDP. We have previously revealed that CD1d-restricted, $V_\alpha 24$–$J_\alpha Q$ NKT cells are remarkably reduced in the peripheral blood from MS. However, $V_\alpha 7.2$–$J_\alpha 33$ T cells are not reduced in the peripheral blood from MS and could be detected in a large majority of the cerebrospinal fluid samples obtained during relapse of MS. The present results indicate that the $V_\alpha 7.2$–$J_\alpha 33$ T cells are involved in the autoimmune inflammatory lesions.

Introduction

Conventional T cells display a wide and diverse repertoire with regard to TCR that are made by random recombination of V, D and J segments as well as junctional deletion and insertion of nucleotides. In addition to these mainstream T cells that have undergone thymic selection for cognate peptides bound to MHC molecules, there also exist discrete 'invariant' lymphocyte populations, characterized by limited repertoire diversity due to their expression of an invariant receptor chain (1). The most well-characterized 'invariant' T cells are CD1d-rectricted NKT cells, which constitute a major component of lymphocyte populations expressing TCR and NK cell markers. The NKT cells are reactive to glycolipid presented by CD1d molecules and express an invariant TCR α chain paired with particular V_β segments [$V_\alpha 24$–$J_\alpha Q$ α chain paired with $V_\beta 11$ in humans; $V_\alpha 14$–$J_\alpha 281$ with $V_\beta 8.2$ and 7 in rodents] (2–4). Although the natural ligand for the CD1d-restricted NKT cells still remains unknown, they could produce large amounts of cytokines shortly after TCR ligation, allowing us to speculate that they play a critical role in regulation of various immune responses that would maintain the state of health or cause damage to self-tissues.

Correspondence to: T. Yamamura; E-mail: yamamura@ncnp.go.jp

Transmitting editor: L. Steinman

Received 26 June 2003, *accepted* 17 October 2003

Several lines of evidence indicate that the T cell repertoire in humans contains 'invariant' T cells distinct from CD1d-restricted NKT cells (2,5–7). It has recently been proposed that T cells expressing an invariant AV19–AJ33 TCR (the canonical $hV_\alpha 7.2$–$J_\alpha 33$ or $mV_\alpha 19$–$J_\alpha 33$ TCR rearrangement) represent a second 'invariant' T cell subset that would develop in the absence of CD1d (8–11). Independent studies by Lantz *et al.* (8,11) and Shimamura *et al.* (9,10) have shown that the $V_\alpha 19$–$J_\alpha 33$ T cells do not require CD1d for their development and expansion *in vivo*. They are present in TAP-1 knockout mice (8), but are absent in β_2-microglobulin-deficient mice (8,9), suggesting that they probably recognize a non-peptide antigen associated with a non-classical MHC class Ib molecule other than CD1d. Although surface phenotypes of the invariant T cells remain to be fully characterized, the $V_\alpha 19$–$J_\alpha 33$ T cells were enriched in the $NK1.1^+CD3^+$ population isolated from CD1d-deficient mice (9), allowing us to refer to the 'invariant' T cells as a second type of NKT cells. Very recently, Lantz *et al.* (11) have reported that the 'invariant' T cells are enriched in the gut lamina propria, and that their selection and/or expansion require B cells and commensal flora. The distribution of the cell population would indicate that the novel 'invariant' T cells are possibly involved in the host response at the site of pathogen entry. Finally, MR1, a non-classical class I-related molecule (12), has been identified as a restriction element involved in the selection of the $V_\alpha 19$–$J_\alpha 33$ T cells.

It is of note that the novel MR1-restricted NKT cells share several characteristics with CD1d-resticted NKT cells. For example, both of the 'invariant' populations can be detected in unrelated individuals with different ethnic backgrounds and a majority of the cells resides in the $CD4^-CD8^-$ T cell population (7,8). As noted, the TCR α chain represents the canonical V_α–J_α rearrangement, whereas the β chain sequence is restricted by the use of particular V_β segments ($hV_\beta 11$ for CD1d-restricted NKT cells and $hV_\beta 2$ and 13 for MR1-restricted T cells). Both of the 'invariant' populations have a 'natural' memory phenotype ($CD44^{high}$). Furthermore, the invariant TCR sequences as well as their restriction elements (CD1d and MR1) are highly conserved across the species. These characteristics are consistent with the idea that the 'invariant' lymphocyte populations might exert an immediate response against phylogenetically conserved antigens at the frontier between innate and adaptive immunity (1). In accordance with this idea, CD1d-restricted NKT cells produce large amounts of IL-4 and IFN-γ within hours of TCR engagement (3,13–15). Through the explosive release of cytokines and chemokines, they are capable of initiating a cascade of immunological events involved in regulation of autoimmunity and vital defense against microbial agents or tumor cells (1). In contrast, very little is known about the function of the MR1-resricted T cells. Although accumulating data indicate that they may promptly respond to antigen by producing IL-4 (Shimamura *et al.*, unpublished observations), their ability to produce cytokines and chemokines needs to be systematically analyzed in the coming years.

A numerical reduction or functional alterations in CD1d-rectricted NKT cells bearing the $V_\alpha 24$–$J_\alpha Q$ invariant chain have been documented in various human autoimmune diseases (3,4). Using three different approaches, the RT-PCR single-strand conformation polymorphism (SSCP) clonotype method (16), anti-$V_\alpha 24$ and anti-$V_\beta 11$ antibodies, and glycolipid-loaded CD1d tetramers (17), we have recently revealed that the $V_\alpha 24$–$J_\alpha Q$ NKT cells are greatly reduced in number in the peripheral blood of multiple sclerosis (MS), a putative autoimmune disease mediated by $T_h 1$ autoimmune T cells (18,19). We also examined the distribution of the $V_\alpha 24$–$J_\alpha Q$ NKT cells in the central nervous system (CNS) lesions from patients with MS as well as in the peripheral nerve biopsy samples derived from chronic inflammatory demyelinating polyneuropathy (CIDP) patients (16). Although expression of non-invariant $V_\alpha 24$ rearrangement was ubiquitous in the CNS samples of MS, the $V_\alpha 24$–$J_\alpha Q$ clonotype specific for the NKT cells appeared to be missing in most of the CNS lesions. In contrast, the NKT cell clonotype could be readily detected in a large majority of the biopsy samples of CIDP, which is a chronic demyelinating disease of the peripheral nervous system (PNS) with a presumed autoimmune origin (20).

Using the same samples previously analyzed for the $V_\alpha 24$–$J_\alpha Q$ NKT cells (16), we conducted experiments to address the following questions. (i) Are the invariant $V_\alpha 7.2$–$J_\alpha 33$ T cells reduced in the peripheral blood of MS? (ii) Are they involved in the inflammatory lesions of MS and CIDP or could they be missing from the lesions? (iii) Are they present in the cerebrospinal fluid (CSF) derived from MS? Here, we report that unlike the $V_\alpha 24$–$J_\alpha Q$ NKT cells, the $V_\alpha 7.2$–$J_\alpha 33$ T cells are not reduced in the peripheral blood of MS. More strikingly, they were detected in some of the pathological samples obtained from MS and in the majority of nerve biopsy samples from CIDP, and could be detected in the CSF samples from MS. Comparison with other T cell populations indicated a selective accumulation of the $V_\alpha 7.2$–$J_\alpha 33$ T cells in the inflammatory lesions. We propose that the invariant $V_\alpha 7.2$–$J_\alpha 33$ T cells do not only play a role in protection against pathogen entry in the gut (11), but also in the regulation of autoimmune tissue inflammation.

Methods

Selection of patients with MS or CIDP

We obtained peripheral blood and CSF from patients with 'definite MS' according to the diagnostic criteria proposed by Poser *et al.* (21). The diagnosis of MS was further assisted by magnetic resonance imaging and evoked responses. All patients had remitting-relapsing MS and did not receive immunosuppressive agents at the time of investigation. Diagnosis of CIDP was based on the criteria of the American Academy of Neurology (22).

Peripheral blood mononuclear cells (PBMC), CSF, CNS and PNS samples

Heparinized blood (20 ml) was taken and PBMC were isolated by Ficoll density gradient centrifugation. CSF samples were obtained within 1 week after the onset of exacerbation. The sural nerve biopsy samples were taken for other diagnostic purposes with standard procedure (23). Samples were snap-frozen and were stored at −70°C along with frozen brain samples until analysis had been performed. The histopatho-

logical characterization of the MS plaques was performed as described previously (24).

Isolation of mRNA and synthesis of cDNA

mRNAs were isolated from 10^7 PBMC and from CSF sediment using the QuickPrep Micro mRNA purification kit (Amersham-Pharmacia Biotech, Uppsala, Sweden). The air-dried pellet was resuspended in 20 µl of RNase-Free Water and used for cDNA synthesis by the First-Strand cDNA synthesis kit (Amersham-Pharmacia Biotech, Uppsala, Sweden) using oligo-dT as primer. The mRNAs previously isolated from autopsy CNS samples and sural nerve biopsy samples (16) were also converted to cDNA by the same approach.

SSCP analysis

We conducted RT-PCR SSCP following amplification with V_α and C_α primers as described previously (16,25). Primers and probes were designed based on the previously published sequences (2,3,5,8,26). To detect the $V_\alpha 7.2$–$J_\alpha 33$ invariant chain, 1 µl of the diluted cDNA was used for each PCR reaction with $V_\alpha 7.2$-specific sense primer (GTCGGTCTAAAGGGTACAGT) and anti-sense C_α-specific primer (CAGCTGAGAGACTCTAAAT). cDNAs obtained from PBMC samples were amplified by PCR for 39 cycles, while cDNAs from autopsy/biopsy samples and CSF were amplified for 40 cycles. Quantities of 0.2 µg of sense and 0.2 µg of anti-sense primers (30 pmol) were added to 50-µl reactions containing 5 µl of 10 × ExTaqBuffer, dNTPs and 2.5 U of ExTaq DNA polymerase (Takara, Tokyo, Japan). Amplified DNAs were diluted (1:3) and heat-denatured. Aliquots of 4 µl of the diluted samples were electrophoresed in non-denaturing 4% polyacrylamide gel. DNAs were transferred to Immobilon-S (Millipore Intertech, Bedford, MA) and hybridized with biotinylated C_α-specific (AAATATCCAGAACCCTGACCCTGCCGTGTACC), $J_\alpha 33$-specific (TATCAGTTAATCTGGGGCGCTGGGACCAAGCT) or invariant $V_\alpha 7.2$–$J_\alpha 33$-specific internal probe (TGTGCTGTGAGAGATAGCAACTATCAGTTAATCTG). To detect the $V_\alpha 24$–$J_\alpha Q$ invariant chain, cDNAs were PCR amplified with $V_\alpha 24$-specific sense primer (ACACAAAGTCGAACGGAAG) and C_α-specific anti-sense primer (GATTTAGAGTCTCTCAGCTG), and then hybridized with a probe specific for the invariant $V_\alpha 24$–$J_\alpha Q$ sequence (TGTGTGGTGAGCGACAGAGGCTCAACCCTG) as previously described (16).

SSCP clonotypes were visualized by incubation with streptavidin, biotinylated alkaline phosphatase and a chemiluminescent substrate system (Phototope; New England Biolabs, Bedford, MA). cDNAs for human IL-4 and IFN-γ were amplified by RT-PCR as described previously (16).

Real-time $V_\alpha 7.2$ clonotypic RT-PCR

Quantitative RT-PCR (LightCycler; Roche Molecular Biochemicals, Mannheim, Germany) was performed with the $V_\alpha 7.2$ sense primer and with an anti-sense primer matching the CDR3α region of the $V_\alpha 7.2$–$J_\alpha 33$ T cells (TGATAGTTGCTATCTCTCAC). An aliquot of 1 µl of the cDNA was amplified by PCR for 40 cycles using quantification with a commercial kit (LightCycler DNA Master SYBR Green I; Roche Molecular Biochemicals). Quantities of 0.2 µg of sense and 0.2 µg of anti-sense primers (30 pmol) were added to 50-µl reactions containing 5 µl of 10 × ExTaqBuffer, dNTPs and 2.5 U of ExTaq DNA polymerase (Takara). All PCR reactions were controlled by β-actin expression (sense primer: AGAGATGGCCACGGCTGCTT; anti-sense primer: ATTTGCGGTGGACGATGGAG) (27). Based on the standard values of control samples, the relative expression for each sample was determined with the LightCycler software.

TCR DNA sequencing

In brief, small areas of the SSCP gel corresponding to the clonotypes of interest were cut out and DNAs were eluted as described previously (25). A second PCR was performed with the corresponding V_α-specific and C_α-specific primers using the eluted DNAs as template. The PCR products were cloned into pCR 2.1-TOPO Vector using TOPO TA cloning kit (Invitrogen, Carlsbad, CA) and recombinants were sequenced using an ABI 377 DNA sequencer (Applied Biosystems, Foster City, CA).

Results

Invariant $V_\alpha 7.2$–$J_\alpha 33$ T cells represent a dominant $V_\alpha 7.2^+$ subset in the peripheral blood of healthy subjects (HS)

First, we examined if the RT-PCR SSCP clonotype method (16,25,28,29) could be used to detect the invariant $V_\alpha 7.2$–$J_\alpha 33$ sequence in peripheral blood derived from HS. Following mRNA isolation from nine PBMC samples, the TCR α chain sequences encompassing the αCDR3 region were RT-PCR amplified with a set of $V_\alpha 7.2$ and C_α primers. The amplified cDNAs were denatured and electrophoresed on the SSCP gel, and hybridized with C_α-, $J_\alpha 33$- or invariant $V_\alpha 7.2$–$J_\alpha 33$-specific probe. Hybridization with the C_α probe has revealed several bands in the smear background on the gel, indicating that T cells using the $V_\alpha 7.2$ segment are restricted, but heterogeneous (Fig. 1, upper panel). However, hybridizing with the $J_\alpha 33$ probe revealed a solitary band in each sample at a same position (Fig. 1, middle panel), indicating that a single clonotype may dominate the TCR $V_\alpha 7.2$ and $J_\alpha 33$ rearrangements found in the peripheral blood. Given that the invariant $V_\alpha 7.2$–$J_\alpha 33$ clonotype was identified as an expanded clonotype in prior studies (7,8), we speculated that the solitary band that hybridized with the $J_\alpha 33$-specific probe might correspond to the invariant $V_\alpha 7.2$–$J_\alpha 33$ sequence. Consistent with this speculation, the invariant $V_\alpha 7.2$–$J_\alpha 33$-specific probe detected a distinct band at the same position where the $J_\alpha 33$-specific probe hybridized (Fig. 1, lower panel).

To confirm if the clonotype hybridized with the $J_\alpha 33$-specific probe represents the invariant $V_\alpha 7.2$–$J_\alpha 33$, we eluted DNA from the sites of the gel corresponding to the band, and amplified the DNA by a second PCR with $V_\alpha 7.2$ and C_α primers. The amplified cDNAs were cloned and 10–15 clones from each individual were sequenced. Analysis of four randomly selected HS has shown that 70–90% of the clones from each subject possess the $V_\alpha 7.2$–$J_\alpha 33$ invariant sequence (GTG AGA) in the CDR3 region. Another CDR3 DNA sequence (GTG ATG combined with $J_\alpha 33$) was detected repeatedly in two of the four individuals. However, all the other sequences differed from each other and were not shared by different individuals. This analysis assured that the solitary band of our

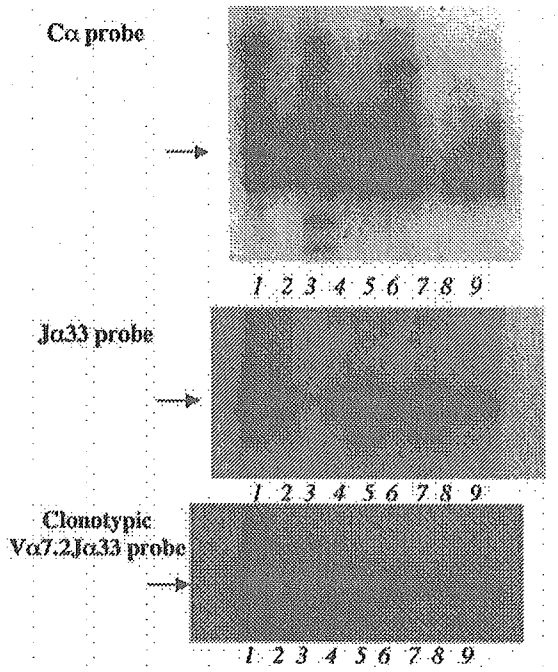

Fig. 1. Detection of the invariant $V_\alpha 7.2$–$J_\alpha 33$ TCR in the peripheral blood of HS. The $V_\alpha 7.2^+$ T cell repertoire in the peripheral blood was analyzed with the SSCP technique. The $V_\alpha 7.2^+$ TCR amplified from nine HS were hybridized with the C_α-specific probe (upper panel), the $J_\alpha 33$-specific probe (middle panel) or the invariant $V_\alpha 7.2$–$J_\alpha 33$ clonotype-specific probe (lower panel). Arrows indicate the position for the invariant $V_\alpha 7.2$–$J_\alpha 33$ clonotype. The numerical code corresponds to each subject.

interest corresponds to the clonotype expressed by the MR1-restricted T cells.

Invariant $V_\alpha 7.2$–$J_\alpha 33$ T cells do not expand in response to α-galactosylceramide (α-GalCer)

$V_\alpha 24$–$V_\alpha 11$ NKT cells are known to proliferate in response to α-GalCer, which is a prototype ligand for the NKT cells (4,17). Additionally, we examined if the invariant $V_\alpha 7.2$–$J_\alpha 33$ T cells respond to α-GalCer. In brief, PBMC from healthy individuals were stimulated with α-GalCer as previously described (17) and the α-GalCer-stimulated PBMC cultures were harvested at different time points for SSCP analysis. We observed that the invariant $V_\alpha 7.2$–$J_\alpha 33$ clonotype would gradually diminish, while the $V_\alpha 24$–$V_\alpha 11$ clonotype remarkably expanded shortly after stimulation with α-GalCer (data not shown). This result confirms that α-GalCer is not a stimulatory ligand for the invariant $V_\alpha 7.2$–$J_\alpha 33$ T cells.

Invariant $V_\alpha 7.2$–$J_\alpha 33$ T cells are not reduced in the peripheral blood of MS

In previous studies, we have demonstrated that the $V_\alpha 24$–$J_\alpha Q$ NKT cells are remarkably reduced in the peripheral blood of MS, particularly in the remission phase (16,17). In fact, SSCP analysis for the $V_\alpha 24$–$J_\alpha Q$ clonotype detected the NKT cell clonotype in all the HS (18 of 18, 100%) (16), but the clonotype was not found in any of the MS patients in remission (Table 1).

Table 1. Detection frequency of the invariant $V_\alpha 7.2$–$J_\alpha 33$ TCR versus invariant $V_\alpha 24$–$J_\alpha Q$ TCR in various samples

	$V_\alpha 7.2$–$J_\alpha 33$	$V_\alpha 24$–$J_\alpha Q$
PBMC-HS	9/9 (9)	18/18 (18)
PBMC-MS	13/15 (15)	0/18 (18)
CNS-MS	7/14 (7)	1/14 (8)
CNS-control	1/6 (1)	0/6 (0)
CSF-MS	8/11 (10)	11/24 (24)
PNS-CIDP	8/10 (10)	6/10 (10)
PNS-OND	0/11 (4)	0/11 (4)

Using the SSCP clonotype method, we have previously examined the presence of the $V_\alpha 24$–$J_\alpha Q$ clonotype in various types of samples (16). Here we evaluated the presence of the $V_\alpha 7.2$–$J_\alpha 33$ clonotype in the same samples with a similar methodology. Data represent the number of samples containing the invariant TCR/the total number of samples. In the parentheses, we give the number of samples from which $V_\alpha 7.2^+$ or $V_\alpha 24^+$ TCR could be amplified.
The examined samples include PBMC from HS (PBMC-HS) or from MS in remission (PBMC-MS), CNS plaques from MS (CNS-MS), CNS samples from autopsy cases without neurological disease (CNS-control), CSF samples from MS during relapse (CSF-MS), and sural nerve biopsy samples from CIDP (PNS-CIDP) and from other neurological disease (PNS-OND).

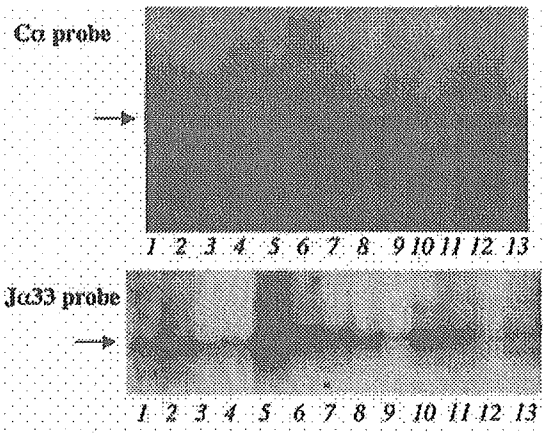

Fig. 2. Detection of the invariant $V_\alpha 7.2$–$J_\alpha 33$ TCR in the peripheral blood of MS. The $V_\alpha 7.2^+$ TCR amplified from the peripheral blood of 15 MS patients were analyzed by SSCP followed by hybridization with a C_α (upper panel)- or $J_\alpha 33$ (lower panel)-specific probe. Thirteen out of the 15 samples displayed the invariant clonotype (arrow). The presence of clonotypes distinct from the invariant $V_\alpha 7.2$–$J_\alpha 33$ clonotype indicates expansion of conventional $V_\alpha 7.2^+$ T cells. See also Table 1 summarizing the pooled data.

Given the notable similarities between CD1d-restricted NKT cells and MR1-resricted T cells, we speculated that the invariant $V_\alpha 7.2$–$J_\alpha 33$ clonotype might also be reduced in the peripheral blood of MS. However, the invariant clonotype could be readily detected by the SSCP method in 13 of 15 peripheral blood samples from MS patients in remission (Fig. 2 and Table 1). To further evaluate the frequency of the $V_\alpha 7.2$–$J_\alpha 33$ T cells in PBMC of MS, we applied a real-time RT-PCR with $V_\alpha 7.2$- and $V_\alpha 7.2$–$J_\alpha 33$ clonotype-specific primers for quantitative analysis. Using this assay, we measured relative

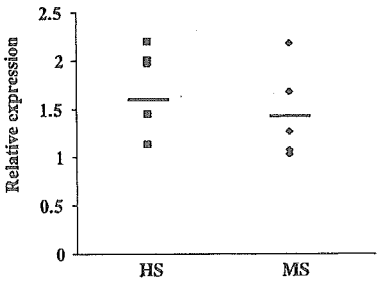

Fig. 3. Real-time RT-PCR assay for the invariant $V_\alpha 7.2$–$J_\alpha 33$ TCR. Expression of the invariant $V_\alpha 7.2$–$J_\alpha 33$ mRNA in the peripheral blood was quantitatively analyzed by applying quantitative RT-PCR (LightCycler). The PBMC from five HS and five MS were examined, and expression of the invariant $V_\alpha 7.2$–$J_\alpha 33$ TCR was quantified in comparison to that of β-actin. The values represent relative expression of the invariant TCR in each sample, where the lowest value is indicated as 1. The horizontal lines show the mean (HS 1.726 ± 0.44, MS 1.416 ± 0. 48).

expression of the invariant $V_\alpha 7.2$–$J_\alpha 33$ mRNA in the PBMC derived from five MS in remission and from five HS. As shown in Fig. 3, there was no significant difference between HS and the patients with MS. Taken together, we conclude that MR1-restricted T cells are conserved in number in the patients with MS.

Infiltration of the invariant $V_\alpha 7.2$–$J_\alpha 33$ T cells in the CIDP lesions

We could previously demonstrate an expression of the invariant $V_\alpha 24$–$J_\alpha Q$ TCR in 60% of the peripheral nerve biopsy samples from CIDP (16). A possible interpretation was that the NKT cells may be recruited to the lesions like inflammatory cells (30–32). It is very interesting to know if MR1-restricted T cells are also recruited to the CIDP lesions. Here we examined the CIDP samples for their expression of the $V_\alpha 7.2$–$J_\alpha 33$ invariant sequence. We were able to amplify $V_\alpha 7.2^+$ TCR messages from all the 10 samples. Hybridization with the C_α-specific probe (Fig. 4A) revealed a number of bands in every lesion, suggesting that not only the invariant $V_\alpha 7.2$–$J_\alpha 33$, but conventional $V_\alpha 7.2^+$, T cells may also be present in the lesions. Hybridization with $J_\alpha 33$- or invariant $V_\alpha 7.2$–$J_\alpha 33$-specific probe displayed the invariant clonotype in eight out of the 10 samples (Fig. 4A, and Tables 1 and 2). We also examined 11 nerve biopsy samples from other neurological diseases (OND) as controls. A faint single band was found in four of the 11 OND samples after hybridization with the C_α-specific probe (Fig. 4B). However, none of the samples hybridized with the $J_\alpha 33$-specific probe, excluding the presence of the invariant $V_\alpha 7.2$–$J_\alpha 33$ T cells in the control PNS lesions. These results demonstrate that not only the $V_\alpha 24$–$J_\alpha Q$ NKT cells, but also $V_\alpha 7.2$–$J_\alpha 33$ T cells, would preferentially accumulate in the inflammatory lesions of CIDP.

We classified the CIDP biopsy samples into four groups, based on the expression pattern of the $V_\alpha 7.2$–$J_\alpha 33$ and $V_\alpha 24$–$J_\alpha Q$ invariant sequences (Table 2). Eight of the 10 samples belonged to Group I ($V_\alpha 7.2$–$J_\alpha 33^+/V_\alpha 24$–$J_\alpha Q^+$) or Group II ($V_\alpha 7.2$–$J_\alpha 33^+/V_\alpha 24$–$J_\alpha Q^-$), as reflected by the frequent detection of the $V_\alpha 7.2$–$J_\alpha 33$ clonotype. We could consistently detect IL-4 mRNA in all the samples from Groups I and II. More

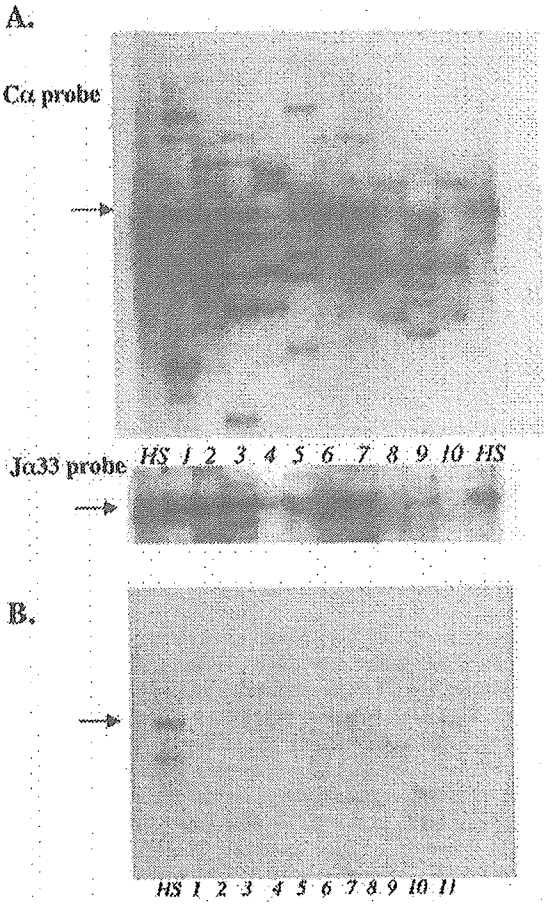

Fig. 4. Demonstration of the $V_\alpha 7.2^+$ TCR rearrangements and the invariant $V_\alpha 7.2$–$J_\alpha 33$ TCR in nerve biopsy samples. (A) Sural nerve biopsy samples from 10 CIDP patients were examined by SSCP. Amplified $V_\alpha 7.2^+$ TCR were hybridized with C_α- and $J_\alpha 33$-specific probes. HS indicates a lane for PBMC from HS, illustrating the position of the invariant $V_\alpha 7.2$–$J_\alpha 33$ clonotype (arrow). The numerical code corresponds to each biopsy sample. The same sample codes are used here and in Table 2. (B) Sural nerve biopsy samples from patients with OND were examined by SSCP. C_α-specific hybridization detected bands in four samples as shown here. However, the $J_\alpha 33$-specific probe did not detect any band (not shown). The OND include hereditary motor and sensory neuropathy, alcoholic polyneuropathy, acute demyelinating polyneuropathy, Churg–Strauss syndrome, POEMS syndrome, diabetic polyneuropathy, and Krabbe disease.

interestingly, IFN-γ was detected in four of five samples from Group I, but detected in only one of three samples from Group II. Although the number of samples was not large enough to draw any conclusion, this may indicate a possible difference between Groups I and II with regard to the cytokine milieu.

Accumulation of the invariant $V_\alpha 7.2$–$J_\alpha 33$ T cells in the autopsy CNS lesions of MS

Next we asked if the $V_\alpha 7.2$–$J_\alpha 33$ T cells may infiltrate into the autopsy CNS lesions of MS. Using the SSCP clonotype method, we analyzed 14 CNS lesions obtained from five

Table 2. Classification of the CIDP lesions based on the expression pattern of the invariant TCR

	V_α7.2–J_α33	V_α24–J_αQ	IFN-γ	IL-4
Group I				
CIDP-1	+	+	+	+
CIDP-3	+	+	+	+
CIDP-7	+	+	+	+
CIDP-9	+	+	+	+
CIDP-5	+	+	−	+
Group II				
CIDP-2	+	−	−	+
CIDP-4	+	−	−	+
CIDP-6	+	−	+	+
Group III				
CIDP-8	−	+	−	+
Group IV				
CIDP-10	−	−	+	−

The sural nerve lesions derived from CIDP were classified into four groups based on the expression pattern of the invariant TCR of the MR1-restricted T cells and of CD1d-restricted NKT cells. Here we define those expressing both of the invariant chains as Group I and those missing both as Group IV. Lesions expressing V_α7.2–J_α33 only or V_α24–J_αQ alone were classified as Groups II and III respectively. Expression of IFN-γ and IL-4 was detected by RT-PCR.

autopsied cases with MS, including seven acute plaques, six subacute plaques and one chronic plaque. V_α7.2$^+$ TCR could be amplified by RT-PCR from seven out of the 14 lesions, although they were detected only in one of the six control CNS samples (Table 1). We found that all the V_α7.2$^+$ plaques (four acute plaques, two subacute plaques and a single chronic plaque) expressed the message for the invariant V_α7.2–J_α33 sequence (Fig. 5, upper panel and Table 1). In contrast, as reported previously (16), whereas Vα24$^+$ TCR could be amplified from eight of the 14 MS autopsy lesions, only a single subacute plaque expressed the V_α24–J_αQ clonotype, i. e. the invasion of V_α24–J_αQ NKT cells was mainly restricted to the CIDP lesions, whereas the V_α7.2–J_α33 T cells were also found in some CNS lesions from MS. To verify the postulate that the V_α7.2–J_α33 T cells are involved in the pathology of MS, we also analyzed CSF samples obtained at an acute stage of MS. We were able to detect the V_α7.2–J_α33 invariant sequence in 73% of the samples examined (Fig. 5, lower panel and Table 1), supporting that the invariant V_α7.2–J_α33 T cells are a component of the CNS infiltrates in MS.

In parallel to V_α7.2$^+$ TCR and V_α24$^+$ TCR, we examined the V_α19$^+$ TCR repertoire with the SSCP method. With the C_α-specific probe, we could detect a number of V_α19$^+$ clonotypes in all the PBMC samples obtained from HS and MS (Table 3). However, V_α19$^+$ TCR was not detected in any of the CNS samples from MS or PNS samples from CIDP. This result indicates that the presence of a particular clonotype in the MS lesions does not simply reflect that this population is present in the peripheral circulation. In other words, it implies that the presence of the V_α7.2–J_α33 clonotype may indicate the 'lesiophilic' nature of the MR1-restricted T cells.

Discussion

It has been demonstrated repeatedly that CD4$^-$CD8$^-$ T cells in the human peripheral blood contain clonally expanded T cell

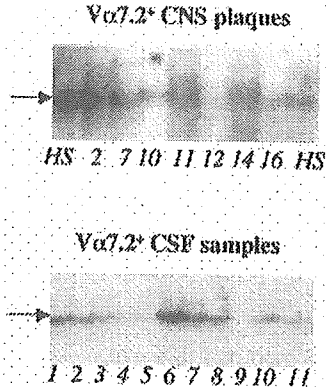

Fig. 5. Demonstration of the invariant V_α7.2–J_α33 TCR in autopsy CNS samples and CSF from MS. Fourteen CNS autopsy samples and 11 CSF samples from MS were analyzed in these experiments. The V_α7.2$^+$ samples were hybridized with a C_α-specific probe and re-hybridized with the invariant V_α7.2–J_α33-specific probe. HS indicates a lane for PBMC from a HS, illustrating the position of the invariant V_α7.2–J_α33 clonotype (arrow).

Table 3. Detection frequency of V_α19$^+$ TCR clonotypes in various samples

PBMC-HS	9/9
PBMC-MS	15/15
CNS-MS	0/14
CNS-control	0/6
PNS-CIDP	0/10
PNS-OND	1/11

Data represent the number of samples containing the V_α19 TCR/the total number of samples. The same samples were used for V_α24–J_αQ and V_α7.2–J_α33 clonotypes (Table 1).

populations (5–8). For example, CDR3 spectratyping analysis for the peripheral CD4$^-$CD8$^-$ T cells in healthy individuals has previously indicated clonal expansion of T cells bearing invariant V_α7.2–J_α33, V_α4–J_α29 or V_α19–J_α48 in addition to those expressing the V_α24–J_αQ NKT cell clonotype (7). After knowing that biopsy samples of CIDP are often infiltrated with the V_α24–J_αQ NKT cells (16), we attempted to analyze the expression of the V_α7.2–J_α33, V_α4–J_α29 and V_α19–J_α48 invariant sequences in the lesions of MS and CIDP. However, the invariant V_α4–J_α29 and V_α19–J_α48 sequences were not detected in any of the samples (data not shown). Accordingly, we focused our efforts on analysis of the V_α7.2–J_α33 T cells. In order to shed light on the difference and similarity between the V_α7.2–J_α33 and V_α24–J_αQ NKT cells, we examined the autopsy and biopsy samples as well as PBMC and CSF samples previously analyzed for the expression of the V_α24–J_αQ TCR (16).

Here, we documented that the autopsy CNS lesions from MS as well as the biopsy PNS lesions from CIDP are infiltrated with the invariant V_α7.2–J_α33 T cells. We also showed that the invariant V_α7.2–J_α33 T cells are present in a large majority of the CSF samples obtained at relapse phases of MS. In contrast, V_α19$^+$ TCR could not be detected in any of the affected tissues from MS or CIDP after PCR amplification,

although they can be detected in all the PBMC samples. Although the function of the invariant $V_\alpha 7.2$–$J_\alpha 33$ T cells remains elusive, the present results demonstrated for the first time to our knowledge that the novel invariant T cells (8–11) are present in autoimmune inflammation affecting the nervous system.

In a very recent report (11), Lantz *et al.* showed that the MR1-restricted invariant T cells are preferentially located in the gut mucosa and therefore proposed to name the population as mucosal-associated invariant T cells (MAIT). In support of the special role of this cell population in the mucosa, the number of the cells in the gut mucosa was greatly reduced in germ-free mice. This observation indicated the role of commensal flora for selection of the invariant T cells. Although an interpretation for this could be that the MR1-resricted T cells would recognize the exogenous antigen bound to MR1, analysis of the T–T hybridomas showed that they could recognize MR1 directly in the absence of bound ligand (11). If this is indeed the case, the MAIT cells could be autoreactive to MR1. To accommodate the autoreactivity with the requirement for commensal flora, it could be speculated that MR1 expression may require some ligand derived from or induced by commensal flora. An alternative possibility is that microbial products may facilitate translocation of MR1 to the cell membrane.

Provided that the invariant $V_\alpha 7.2$–$J_\alpha 33$ T cells are generated or expanded in the mucosa, how would they accumulate into the inflammatory lesions of MS and CIDP? Although this remains a conundrum, we would speculate that inflammation-associated signals such as chemokines play a role in the initial step. In fact, CD1d-restricted NKT cells would behave like inflammatory cells and rapidly accumulate into certain granuloma lesions (30), and they could be detected in non-autoimmune inflammatory lesions (31,32). Given a number of similarities between $V_\alpha 7.2$–$J_\alpha 33$ and $V_\alpha 24$–$J_\alpha Q$ NKT cells, we would postulate that the $V_\alpha 7.2$–$J_\alpha 33$ T cells also might be preferentially recruited to the inflammatory sites. To support this idea, non-autoimmune inflammatory lesions are reported to express the invariant $V_\alpha 7.2$–$J_\alpha 33$ TCR (32).

The second critical step may be the interaction of the invariant T cells with B cells expressing MR1 in the site of lesions, given that the vast majority of the inflammatory lesions are infiltrated with B cells. We could expect the $V_\alpha 7.2$–$J_\alpha 33$ T cells to regulate local immune responses by producing cytokines. If IL-4 is the major cytokine produced by the novel invariant T cells, their interaction with B cells may lead to augmentation of antibody production. Even though the encephalitogenic T_h1 autoreactive T cells are down-regulated by IL-4, the direct interaction between B cells and the $V_\alpha 7.2$–$J_\alpha 33$ T cells may substantially augment the tissue damage or alter the type of lesions. However, if suppressive cytokines such as transforming growth factor-β are the major products of the $V_\alpha 7.2$–$J_\alpha 33$ T cells *in vivo*, they may down-regulate the B cells as well as inflammatory cells in the vicinity. Although we can only speculate about how they would deal with auto-immunity, it is possible that they would play an active role in the regulation of autoimmune inflammation. To verify this hypothesis, we need to systematically analyze the functions of the $V_\alpha 7.2$–$J_\alpha 33$ T cells with regard to ligand recognition and cytokine production. It is also important to know if the presence or absence of the invariant T cells may correlate with the type of pathology. The present data indicate that it is indeed a rewarding attempt.

Acknowledgements

We thank Bernhard Greve and Joel Stern for comments on the manuscript and for discussion. This work was supported by the Organization for Pharmaceutical Safety and Research (OPSR/Kiko).

Abbreviations

α-GalCer	α-galactosylceramide
CIDP	chronic inflammatory demyelinating polyneuropathy
CNS	central nervous system
CSF	cerebrospinal fluid
HS	healthy subject
MAIT	mucosal-associated invariant T cell
MS	multiple sclerosis
OND	other neurological disease
PBMC	peripheral blood mononuclear cell
PNS	peripheral nervous system
SSCP	single-strand conformation polymorphism

References

1 Bendelac, A., Bonneville, M. and Kearney, J. F. 2001. Autoreactivity by design: innate B and T lymphocytes. *Nat. Rev. Immunol.* 1:177.
2 Porcelli, S., Yockey, C. E., Brenner, M. B. and Balk, S. P. 1993. Analysis of T cell antigen receptor (TCR) expression by human peripheral blood CD4$^-$CD8$^-$ α/βT cells demonstrates preferential use of several V_α genes and an invariant TCRα chain. *J. Exp. Med.* 178:1.
3 Wilson, S. B. and Delovitch, T. L. 2003. Janus-like role of regulatory iNKT cells in autoimmune disease and tumour immunity. *Nat. Rev. Immunol.* 3:211.
4 Taniguchi, M., Harada, M., Kojo, S., Nakayama, T. and Wakao, H. 2003. The regulatory role of $V_\alpha 14$ NKT cells in innate and acquired immune response. *Annu. Rev. Immunol.* 21:483.
5 Dellabona, P., Padovan, E., Casorati, G., Brockhaus, M. and Lanzavecchia, A. 1994. An invariant $V_\alpha 24$–$J_\alpha Q/V_\beta 11$ T cell receptor is expressed in all individuals by clonally expanded CD4$^-$CD8$^-$ T cells. *J. Exp. Med.* 180:1171.
6 Lantz, O. and Bendelac, A. 1994. An invariant T cell receptor α chain is used by a unique subset of MHC class I-specific CD4$^+$ and CD4$^-$8$^-$ T cells in mice and humans. *J. Exp. Med.* 180:1097.
7 Han, M., Harrison, L., Kehn, P., Stevenson, K., Currier, J. and Robinson, M. A. 1999. Invariant or highly conserved TCR α are expressed on double-negative (CD3$^+$CD4$^-$CD8$^-$) and CD8$^+$ T cells. *J. Immunol.* 163:301.
8 Tilloy, F., Treiner, E., Park, S. H., Garcia, C., Lemonnier, F., de la Salle, H., Bendelac, A., Bonneville, M. and Lantz, O. 1999. An invariant T cell receptor α chain defines a novel TAP-independent major histocompatibility complex class 1b-restricted α/βT cell subpopulation in mammals. *J. Exp. Med.* 189:1907.
9 Shimamura, M. and Huang, Y. Y. 2002. Presence of a novel subset of NKT cell bearing an invariant $V_\alpha 19$. 1–$J_\alpha 26$ TCR alpha chain. *FEBS Lett.* 516:97.
10 Shimamura, M., Huang, Y. Y., Kobayashi, K., Okamoto, N., Goji, H. and Kobayashi, M. 2002. Characterization of a novel NKT cell repertoire expressing an invariant $V_\alpha 19$–$J_\alpha 26$ TCR α chain using the invariant TCR transgenic mice. Presented at *2nd Int. Workshop on CD1 Antigen Presentation and NKT Cells,* abstr. 4. Woods Hole, MA.
11 Treiner, E., Duban, L., Bahram, S., Radosavljevic, M., Wanner, V., Tilloy, F., Affaticati, P., Gilfillan, S. and Lantz, O. 2003. Selection of evolutionarily conserved mucosal-associated invariant T cells by MR1. *Nature* 422:164.
12 Hashimoto, K., Hirai, M. and Kurosawa, Y. 1995. A gene outside

the human MHC class I-like molecule in T cell activation. *Science* 269:693.

13 Yoshimoto, T. and Paul, W. E. 1994. $CD4^{pos}$, $NK1.1^{pos}$ T cells promptly produce interleukin 4 in response to *in vivo* challenge with anti-CD3. *J. Exp. Med.* 179:1285.

14 Chen, H. and Paul, W. E. 1997. Cultured $NK1.1^+CD4^+$ T cells produce large amounts of IL-4 and IFN-γ upon activation by anti-CD3 or CD1. *J. Immunol.* 159:2240.

15 Miyamoto, K., Miyake, S. and Yamamura, T. 2001. A synthetic glycolipid prevents autoimmune encephalomyelitis by inducing T_h2 bias of natural killer cells. *Nature* 413:531.

16 Illés, Z., Kondo, T., Newcombe, J., Oka, N., Tabira, T. and Yamamura, T. 2000. Differential expression of NK T cell $V_\alpha 24J_\alpha Q$ invariant TCR chain in the lesions of multiple sclerosis and chronic inflammatory demyelinating polyneuropathy. *J. Immunol.* 164:4375.

17 Araki, M., Kondo, T., Gumperz, J. E., Brenner, M. B., Miyake, S. and Yamamura, T. 2003. T_h2 bias of $CD4^+$ NKT cells derived from multiple sclerosis in remission. *Int. Immunol.* 15:279.

18 Martin, R., Ruddle, N. H., Reingold, S. and Hafler, D. A. 1998. T helper cell differentiation in multiple sclerosis and autoimmunity. *Immunol. Today* 19:495.

19 Steinman, L. 2001. Multiple sclerosis: a two-stage disease. *Nat. Immunol.* 2:762.

20 Kieseier, B. C., Dalakas, M. C. and Hartung, H. P. 2002. Immune mechanisms in chronic inflammatory demyelinating neuropathy. *Neurology* 59:S7.

21 Poser, C. M., Paty, D. W., Scheinberg, L., MacDonald, W. I., Davis, F. A., Ebers, G. C., Johnson, K. P., Sibley, W. A., Silberberg, D. H. and Tourtellotte, W. W. 1983. New diagnostic criteria for multiple sclerosis: guidelines for research protocols. *Ann. Neurol.* 13:227.

22 Ad Hoc Subcommittee of the American Academy of Neurology AIDS Task Force. 1991. Research criteria for diagnosis of chronic inflammatory demyelinating polyneuropathy (CIDP). *Neurology* 41:617.

23 Dyck, P. J., Thomas P. K. and Griffin J. W., eds. 1993. *Peripheral Neuropathy*, 3rd edn. Saunders, Philadelphia, PA.

24 Li, H., Newcombe, J., Groome, N. and Cuzner, M. L. 1993. Characterization and distribution of phagocytic macrophages in multiple sclerosis plaques. *Neuropathol. Appl. Neurobiol.* 19:214.

25 Illés, Z., Kondo, T., Yokoyama, K., Ohashi, T., Tabira, T. and Yamamura, T. 1999. Identification of autoimmune T cells among *in vivo* expanded $CD25^+$ T cells in multiple sclerosis. *J. Immunol.* 162:1811.

26 Arden, B., Clark, S., Kabelitz, D. and Mak, T. W. 1995. Human T cell receptor variable gene segment families. *Immunogenetics* 42:455.

27 Takahashi, K., Miyake, S., Kondo, T., Terao, K., Hatakenaka, M., Hashimoto, S. and Yamamura, T. 2001. Natural killer type 2 bias in remission of multiple sclerosis. *J. Clin. Invest.* 107:23.

28 Yamamoto, K., Masuko-Hongo, K., Tanaka, A., Kurokawa, M., Hoeger, T., Nishioka, K. and Kato, T. 1996. Establishment and application of a novel T cell clonality analysis using single-strand conformation polymorphism of T cell receptor messenger signals. *Hum. Immunol.* 48:23.

29 Nam, K. H., Illés, Z., Terao, K., Yoshikawa, Y. and Yamamura, T. 2000. Characterization of expanded T cell clones in healthy macaques: ontogeny, distribution and stability. *Dev. Comp. Immunol.* 24:703.

30 Mempel, M., Ronet, C., Suarez, F., Gilleron, M., Puzo, G., Van Kaer, L., Lehuen, A., Kourilsky, P. and Gachelin, G. 2002. Natural killer T cells restricted by the monomorphic MHC class 1b CD1d1 molecules behave like inflammatory cells. *J. Immunol.* 168:365.

31 Yamazaki, K., Ohsawa, Y. and Yoshie, H. 2001. Elevated proportion of natural killer T cells in periodontitis lesions. *Am. J. Pathol.* 158:1391.

32 Mempel, M., Flageul, B., Suarez, F., Ronet, C., Dubertret, L., Kourilsky, P., Gachelin, G. and Musette, P. 2000. Comparison of the T cell patterns in leprous and cutaneous sarcoid granulamas. Presence of $V_\alpha 24$-invariant natural killer T cells in T-cell-reactive leprosy together with a highly biased T cell receptor V_α repertoire. *Am. J. Pathol.* 157:509.

Research article

The clinical implication and molecular mechanism of preferential IL-4 production by modified glycolipid-stimulated NKT cells

Shinji Oki, Asako Chiba, Takashi Yamamura, and Sachiko Miyake

Department of Immunology, National Institute of Neuroscience, National Center for Neuroscience and Psychiatry, Tokyo, Japan.

OCH, a sphingosine-truncated analog of α-galactosylceramide (αGC), is a potential therapeutic reagent for a variety of Th1-mediated autoimmune diseases through its selective induction of Th2 cytokines from natural killer T (NKT) cells. We demonstrate here that the NKT cell production of IFN-γ is more susceptible to the sphingosine length of glycolipid ligand than that of IL-4 and that the length of the sphingosine chain determines the duration of NKT cell stimulation by CD1d-associated glycolipids. Furthermore, IFN-γ production by NKT cells requires longer T cell receptor stimulation than is required for IL-4 production by NKT cells stimulated either with immobilized mAb to CD3 or with immobilized "αGC-loaded" CD1d molecules. Interestingly, transcription of *IFN-γ* but not that of *IL-4* was sensitive to cycloheximide treatment, indicating the intrinsic involvement of de novo protein synthesis for IFN-γ production by NKT cells. Finally, we determined *c-Rel* was preferentially transcribed in αGC-stimulated but not in OCH-stimulated NKT cells and was essential for IFN-γ production by activated NKT cells. Given the dominant immune regulation by the remarkable cytokine production of ligand-stimulated NKT cells in vivo, in comparison with that of (antigen-specific) T cells or NK cells, the current study confirms OCH as a likely therapeutic reagent for use against Th1-mediated autoimmune diseases and provides a novel clue for the design of drugs targeting NKT cells.

Introduction

Natural killer T (NKT) cells are a unique subset of T lymphocytes that coexpress the α/β T cell receptor (TCR) along with markers of the NK lineage such as NK1.1, CD122, and various Ly49 molecules. Most NKT cells express an invariant TCRα chain composed of Vα14-Jα281 segments in mice and Vα24-JαQ segments in humans associated with a restricted set of Vβ genes (1, 2). Unlike conventional T cells, which recognize peptides presented by MHC molecules, NKT cells recognize glycolipid antigens such as α-galactosylceramide (αGC) in the context of a nonpolymorphic MHC class I–like molecule, CD1d (3–5). After being stimulated by a ligand, NKT cells rapidly affect the functions of neighboring cell populations such as T cells, NK cells, B cells, and dendritic cells (6, 7). The various functions of NKT cells are mediated mainly by a rapid release of large amounts of cytokines, including IL-4 and IFN-γ. Whereas IFN-γ provides help for the Th1 responses required for defending against various pathogens and tumors, IL-4 controls the initiation of Th2 responses and has been shown to inhibit Th1-mediated autoimmune responses involved in experimental autoimmune encephalomyelitis (EAE), collagen-induced arthritis (CIA), and type 1 diabetes in NOD mice.

Given the exceptional ability of NKT cells to secrete regulatory cytokines in comparison with that of T cells or NK cells after primary stimulation, we have explored the possibility that ligand stimulation of NKT cells may lead to the suppression of Th1-mediated autoimmune diseases. We have previously demonstrated that OCH, a sphingosine-truncated analog of αGC, preferentially induces Th2 cytokines from NKT cells and that administration of OCH suppresses EAE and CIA by inducing a Th2 bias in autoantigen-reactive T cells (8, 9). However, the molecular mechanism accounting for the unique property of OCH to selectively induce IL-4 has not been clarified yet.

In this study, we used various stimuli, including the prototypic ligand αGC and its derivatives such as OCH, to investigate the molecular basis of the differential production of IL-4 and IFN-γ by NKT cells. We found that OCH, due to its truncated lipid chain, was less stable in binding the CD1d molecule than was αGC and exerted short-lived stimulation on NKT cells. IFN-γ production by NKT cells required longer TCR stimulation than was required for IL-4 production and de novo protein synthesis. *c-Rel* was preferentially transcribed in αGC-stimulated, but not in OCH-stimulated NKT cells and was shown to regulate IFN-γ production by NKT cells. Taken together, these results indicate that sustained TCR stimulation and concomitant c-Rel expression by αGC leads to the production of IFN-γ, whereas short-term activation and marginal *c-Rel* transcription by OCH results in preferential production of IL-4 by NKT cells.

Methods

Mice. C57BL/6 (B6) mice were purchased from CLEA Laboratory Animal Corp. (Tokyo, Japan). MHC class II–deficient I-$A^b\beta^{-/-}$ mice were purchased from Taconic (Germantown, New York, USA). All animals were kept under specific pathogen-free conditions and were used at 7–10 weeks of age. Animal care and use were in accordance with institutional guidelines.

Cell lines, antibodies, plasmids, and reagents. The NKT cell hybridoma (N38.2C12) (10) was a generous gift from K. Hayakawa (Fox Chase Cancer Center, Philadelphia, Pennsylvania, USA) and NS0-derived

Nonstandard abbreviations used: altered glycolipid ligand (AGL); altered peptide ligand (APL); CD28 responsive element (CD28RE); collagen-induced arthritis (CIA); c-Rel lacking C-terminal transactivation domain (c-RelΔTA); cycloheximide (CHX); cyclosporin A (CsA); experimental autoimmune encephalomyelitis (EAE); α-galactosylceramide (αGC); natural killer T (NKT); nuclear factor of activated T cell (NF-AT); phycoerythrin (PE); T cell receptor (TCR).

Conflict of interest: The authors have declared that no conflict of interest exists.

Citation for this article: *J. Clin. Invest.* **113**:1631–1640 (2004). doi:10.1172/JCI200420862.

plasmacytoma cell lines expressing the Kb tail mutant of CD1d (11) were kindly provided by S. Joyce (Vanderbilt University, Nashville, Tennessee, USA). Cells were maintained in RPMI 1640 medium supplemented with 10% FCS, 2 mM L-glutamine, 100 U/ml penicillin/streptomycin, 2 mM sodium pyruvate, and 50 μM β-mercaptoethanol (complete medium). Phycoerythrin (PE)-labeled mAb to NK1.1 (PK136), peridinine chlorophyll protein/cyanine 5.5 -labeled mAb to CD3 (2C11), and recombinant soluble dimeric human CD1d:Ig fusion protein (DimerX I) were from BD PharMingen (San Diego, California, USA). For some experiments mAb's to NK1.1 (PK136) and CD3 (2C11) were conjugated with FITC. Polyclonal antibody to asialo GM_1 was purchased from WAKO Chemicals (Osaka, Japan). The pRc/CMV-c-Rel expression plasmid (12) was a generous gift from Grundström (Umeå University, Umeå, Sweden). The open reading frame of c-Rel cDNA was amplified by PCR and cloned into the retroviral pMIG(W) vector. The forward primer containing the *Xho*I recognition site was 5′-GACTCTCGAGATGGCCTCGAGTGGATATAA-3′ and the reverse primers used for wild-type c-Rel or the dominant negative mutant c-RelΔTA containing *Eco*RI recognition sites were 5′-GACTGAATTCTTATATTTTAAAAAAACCATATGTGAAGG-3′ and 5′-GACTGAATTCTTAACTCGAGATGGACCCGCATG-3′, respectively. The retroviral vector (pMIG) and packaging vector (pCL-Eco) were kindly provided by L. Van Parijs (Massachusetts Institute of Technology, Cambridge, Massachusetts, USA). Cyclosporin A (CsA) and cycloheximide (CHX) were from Sigma-Aldrich (St. Louis, Missouri, USA). All glycolipids were prepared as described in the Supplemental Methods (supplemental material available at http://www.jci.org/cgi/content/full/113/11/1631/DC1). The glycolipids were solubilized in DMSO (100 μg/ml) and were stored at –20°C until use.

Kinetic analysis of glycolipid stability on CD1d molecules. The kinetic analysis of glycolipid stability on CD1d molecules was performed as described previously with slight modifications (13). In brief, the NKT hybridoma was preincubated with 4 μM Fura red and 2 μM Fluo-4 (Molecular Probes, Eugene, Oregon, USA) at room temperature for 45 minutes, washed with RPMI 1640 medium containing 2% FCS (assay media), and resuspended in assay media. For determination of the optimal time for glycolipid loading onto $CD1d^+$ APCs, kinetic analysis was conducted using either αGC or OCH. According to the data obtained in Figure 2C, $CD1d^+$ APCs were pulsed with glycolipids (100 ng/ml) for 30 minutes. Then, cells were washed and resuspended in assay media. Glycolipid-pulsed APCs were harvested every 15 minutes after resuspension, mixed with NKT cells, and subjected to centrifugation in a table-top centrifuge (2,000 *g*) for 60 seconds. Cells were then resuspended briefly and analyzed for calcium influx into NKT hybridoma cells by flow cytometry (EPICS XL; Beckman Coulter, Tokyo, Japan). Activation was expressed as the percentage of Fura-red– and Fluo-4–stained cells in a high-FL1, low-FL4 gate.

In vivo glycolipid treatment and microarray analysis. Mice were injected intraperitoneally with 0.2 ml PBS containing 0.1 mg anti-asialo GM_1 Ab. Forty hours after injection, mice were injected intraperitoneally with αGC, OCH (100 μg/kg), or control vehicle in 0.2 ml PBS. After the indicated time point, liver mononuclear cells or spleen cells were harvested and NKT cells were purified with the AUTOMACS cell purification system using FITC-conjugated mAb to NK1.1 (PK136) and anti-FITC microbeads (Miltenyi Biotech GmbH, Bergisch Gladbach, Germany). The purity of NKT cells in the untreated samples and in the samples treated for 1.5 hours was more than 90%. The purity of the liver-derived samples and spleen-derived samples treated for 12 hours was more than 80% and 74%, respectively. Total RNA isolation with the RNeasy Mini Kit (Qiagen, Chatsworth, California, USA) and whole-microarray procedures using U74Av2 arrays (GeneChip System; Affymetrix, Santa Clara, California, USA) were done according to the manufacturers' instructions. From data image files, gene transcript levels were determined using algorithms in the Gene Chip Analysis Suit software (Affymetrix). Each probe was assigned a "call" of present (expressed) or absent (not expressed) using the Affymetrix decision matrix. Genes were considered to be differentially expressed when (a) expression changed at least threefold in the case of liver NKT–derived samples or twofold in the case of spleen NKT–derived samples compared with the expression in the negative control and (b) increased gene expression included at least one "present call."

In vitro stimulation. Liver mononuclear cells were isolated from B6 mice by Percoll density gradient centrifugation and were stained with PE-NK1.1 and FITC-CD3 mAb's. The $CD3^+NK1.1^+$ cells and $CD3^+NK1.1^-$ cells were sorted with an EPICS ALTRA Cell Sorting System (Beckman Coulter). The purity of the sorted cells was more than 95%. Sorted cells were suspended in RPMI 1640 medium supplemented with 50 μM 2-mercaptoethanol, 2 mM L-glutamine, 100 U/ml penicillin and streptomycin, and 10% FCS and were stimulated with immobilized mAb to CD3. Incorporation of [^{3}H]thymidine (1 μCi/well) for the final 16 hours of the culture was analyzed with a β-1205 counter (Pharmacia, Uppsala, Sweden). We measured the content of cytokines in the culture supernatants by ELISA. For quantitative PCR analysis, we harvested the cells after stimulation with glycolipid to prepare total RNA. Glycolipid stimulation of spleen cells in vitro was done similarly except that 1% syngeneic mouse serum was used instead of FCS. In some experiments, plates were coated with DimerX I (1 μg in 50 μl PBS per well) for 16 hours. After plates were washed extensively with PBS, glycolipids (100–200 ng in 50 μl PBS per well) were added, followed by incubation for another 24 hours. Then, NKT cells were added and cytokine production was analyzed after 72 hours of incubation.

Real-time PCR to monitor gene expression. Real-time PCR was conducted using a Light Cycler-FastStart DNA Master SYBR Green I kit (Roche Diagnostics GmbH, Mannheim, Germany) according to the manufacturer's specifications using 4 mM $MgCl_2$ and 1 pM primers. Values for each gene were normalized to those of a housekeeping gene (*GAPDH*) before the "fold change" was calculated (using crossing point values) to adjust for variations between different samples. Primers used for the analysis of gene expression are described in Supplemental Methods.

ELISA. For evaluation of cytokine production by NKT cells, sorted liver $CD3^+NK1.1^+$ NKT cells were stimulated with immobilized mAb to CD3 in complete medium. The level of cytokine production in cell culture supernatants or in serum was determined by standard sandwich ELISA using purified and biotinylated mAb sets and standards from BD PharMingen. After the addition of a substrate, the reaction was evaluated using a Microplate reader (BioRad).

Retroviral infection of NKT cells. The 293T cells were maintained in DMEM supplemented with 10% FCS, 2 mM L-glutamine, 100 U/ml penicillin/streptomycin, 2 mM sodium pyruvate, and 50 μM β-mercaptoethanol. Liver mononuclear cells were purified and cultured in complete medium supplemented with IL-2 (200 U/ml) for 24–48 hours. Cells were infected with retrovirus prepared by cotransfection of pMIG retroviral vector and pCL-Eco packaging vector into 293T cells. Cells were cultured in complete medium containing IL-2 and IL-15 (50 ng/ml) continuously for 3 days, and

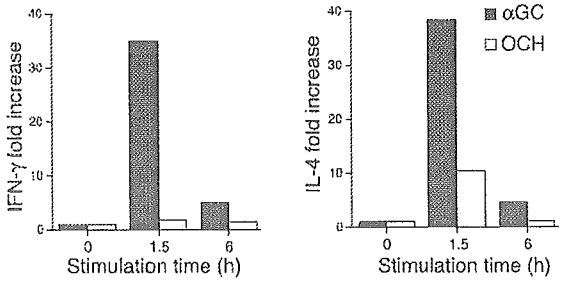

Figure 1
Transcriptional upregulation of cytokine genes by NKT cells stimulated with glycolipids in vivo. B6 mice were injected intraperitoneally with αGC or OCH (100 μg/kg), and liver NKT cells were isolated at the indicated time point. Total RNA was extracted and analyzed for cytokine mRNA by quantitative RT-PCR as described in Methods. Data are presented as "fold induction" of cytokine mRNA after glycolipid treatment. The amount of mRNA in NKT cells derived from untreated animals was defined as 1.

GFP-positive NKT cells were sorted and stimulated with immobilized mAb to CD3 for 48 hours. Culture supernatants were subjected to evaluation of cytokine production by ELISA.

Results

Preferential IL-4 production by OCH-stimulated NKT cells. The suppression of EAE by OCH was found to be associated with a Th2 bias of autoimmune T cells mediated by IL-4 produced by NKT cells (9). To confirm the primary involvement of NKT cells in the Th2 bias seen in the OCH treatment, we purified $CD3^+NK1.1^+$ NKT cells from B6 mice treated in vivo with αGC or OCH and measured the transcription of cytokine genes by quantitative RT-PCR. As shown in Figure 1, treatment with αGC greatly increased the expression of both IFN-γ and IL-4 at 1.5 hours after injection, whereas OCH induced a selective increase in IL-4 expression. When the IL-4/IFN-γ ratio was used for evaluating the Th1/Th2 balance, the NKT cells, isolated at 1.5 hours after injection of OCH were distinctly biased toward Th2 (Table 1). These results indicate that OCH is a selective inducer of rapid IL-4 production by NKT cells when administered in vivo.

Lipid chain length and cytokine production. Comparison of the structural difference between OCH and αGC (Figure 2A) raised the possibility that the lipid chain length of the glycolipid ligand may influence the cytokine profile of glycolipid-treated NKT cells. We compared αGC and OCH as well as newly synthesized analogs F-2/S-3 and F-2/S-7, which bear lipids of intermediate length (Figure 2A), for their ability to induce cytokine production by splenocytes. There was good correlation between the lipid tail length of each glycolipid and its ability to induce IFN-γ from the splenocytes, and a larger amount of IFN-γ was released into the supernatants after stimulation with the glycolipids with the longer sphingosine chain (Figure 2B, right). Regarding the ability to stimulate IL-4 production, the differences among OCH, F-2/S-3 and F-2/S-7 were less clear, as shown by IFN-γ induction. Similar results were obtained with liver mononuclear cells as responder cells (see Supplemental Figure 1). These results indicate that cytokine production by NKT cells, in particular IFN-γ production, is greatly influenced by lipid chain truncation of the glycolipid.

Differential half-life of NKT cell stimulation by CD1d-associated glycolipids. It is believed that the two lipid tails of the glycolipids (sphingosine base and fatty acyl chain) would be accommodated by the highly hydrophobic binding grooves of CD1d. To verify the hypothesis that the functional properties of each glycolipid may be determined by the stability of its binding to CD1d molecules, we evaluated the half-life of these glycolipids on CD1d molecules by estimating calcium influx into NKT hybridoma cells as described previously (13). To exclude the possible involvement of endosomal/lysosomal sorting in this assay, we used APCs expressing a CD1d mutant (Kb tail) that lacks the endosomal/lysosomal targeting signal (11). The cells express both β_2m and sCD1d1 fused to the transmembrane and cytosolic tail sequence of $H\text{-}2K^b$ at the carboxyl terminus and could bind to glycolipids such as αGC or OCH without their internalization and following endosomal/lysosomal sorting. Based on the kinetic analysis data for glycolipid loading efficiency shown in Figure 2C, we pulsed $CD1d^+$ APCs with glycolipids for 30 minutes.

Figure 2D shows that OCH was rapidly released from the CD1d molecule. A 30% reduction in calcium influx was observed after 15 minutes of incubation and only 25% of the initial amount of glycolipid remained after 60 minutes of incubation. In contrast, αGC was not released from CD1d molecule in the first 15 minutes and more than 50% of the initial amount of glycolipid remained after 60 minutes of incubation. F-2/S-3 and F-2/S-7 showed intermediate levels of release from CD1d molecule. These results support the idea that a glycolipid with a shorter sphingosine chain has a shorter half-life for NKT cell stimulation because of less-stable association with the CD1d molecule.

Kinetic analysis of cytokine production by activated NKT cells. Previous in vivo studies demonstrated that injection of αGC into B6 mice can induce a rapid and transient elevation of the serum IL-4 level and a delayed and persistent rise in IFN-γ (9, 14), suggesting that there is an intrinsic difference in kinetics for the production of IL-4 and IFN-γ by NKT cells. To address this issue further, we sorted $CD3^+NK1.1^+$ NKT cells, and conventional $CD3^+NK1.1^-$ T cells as a control, from liver lymphocytes and stimulated the sorted cells with immobilized mAb to CD3 for various periods of time. The cells were then incubated at rest without further stimulation and culture supernatants were harvested at 72 hours after initiation of the TCR stimulation. We found that TCR stimulation of NKT cells for as little as 2 hours could induce detectable IL-4 in the supernatant (Figure 3A, center). The amount of IL-4 in the supernatant rapidly increased in proportion to the duration of TCR stimulation (Figure 3A, center). In contrast, production of IFN-γ by NKT cells required at least 3 hours of TCR stimulation and gradually increased corresponding to the duration of TCR stimulation (Figure 3A, right). Conventional T cells required longer TCR stimulation for efficient cytokine production. We repeatedly confirmed that IFN-γ production by NKT cells required initial stimulation that was 1–2 hours longer and showed a slower accumulation than that of IL-4 production in this experimen-

Table 1
Transcriptional upregulation of cytokine genes by NKT cells stimulated with glycolipids in vivo

Stimulus	Time	*IFN-γ*	*IL-4*	Ratio (*IL-4*/*IFN-γ*)
αGC	1.5 h	35.0	38.3	1.09
	6 h	5.0	4.6	0.92
OCH	1.5 h	1.8	10.3	5.58
	6 h	1.5	1.1	0.72

The relative amounts of transcripts of *IFN-γ* and *IL-4* obtained from the experiment shown in Figure 1 are presented as "fold induction" relative to that of NKT cell–derived samples from untreated animals.

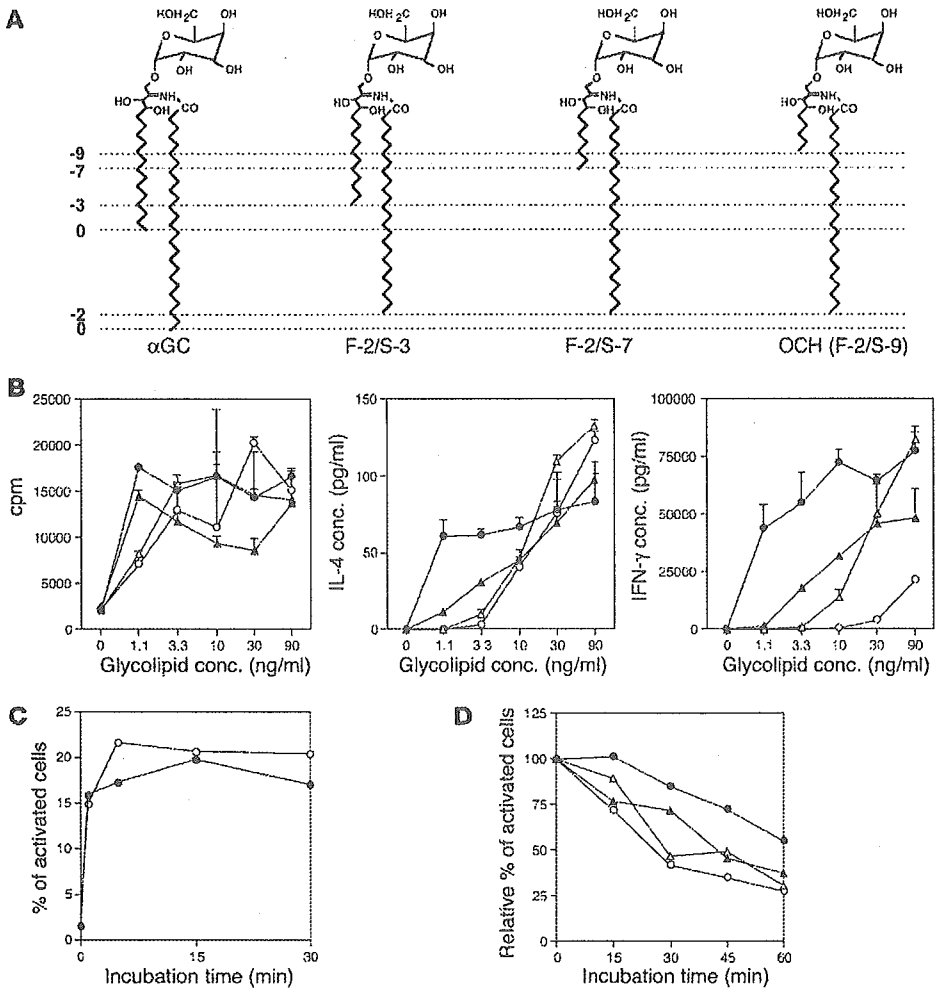

Figure 2

Differential properties of structurally distinct glycolipid derivatives. (**A**) Structures of αGC, OCH, and two other glycolipid ligands for NKT cells. F-2/S-3 has a truncation of two hydrocarbons in the fatty acyl chain (F) and of three hydrocarbons in the sphingosine chain (S) in comparison with αGC. OCH can be called F-2/S-9 accordingly. The numbers of truncated hydrocarbons in either lipid chain are shown along the left margin as negative integers. (**B**) Effect of αGC, OCH, and other glycolipids on proliferation and cytokine production of splenocytes. Splenocytes were stimulated with various concentrations (conc.) of αGC (filled circles), OCH (open circles), F-2/S-3 (filled triangles), or F-2/S-7 (open triangles) for 72 hours. Incorporation of [^{3}H]thymidine (1 μCi/well) during the final 16 hours of the culture was assessed (left), and IL-4 (center) or IFN-γ (right) in the supernatants was measured by ELISA. (**C**) Kinetic analysis of the loading of αGC (filled circles) or OCH (open circles) onto CD1d$^+$ APCs. See Methods for details. One experiment representative of two independent experiments with similar results is shown. (**D**) Calcium influx into NKT hybridoma cells after coculture with CD1d$^+$ APCs pulsed with αGC, OCH, F-2/S-3, or F-2/S-7. Data are presented as the activity remaining when the respective activity of glycolipid-loaded APCs for activation of the NKT cell hybridoma at time 0 was defined as 100%. Data are representative of three experiments with similar results.

tal setting. A similar kinetic difference was also observed when we used spleen-derived NKT cells (data not shown). These results indicate that NKT cells could produce IL-4 after a shorter period of TCR stimulation than is required for IFN-γ production.

To exclude the possibility that a qualitatively different CD1d complex with either αGC or OCH may bind with altered affinity to the TCR, we stimulated NKT cells with plate-bound αGC-CD1d complexes instead of mAb to CD3 for the periods of time indicated in Figure 3B. Consistent with the previous results obtained with anti-CD3 stimulation, the level of IL-4 in the culture supernatant was increased after shorter periods of incubation. In contrast, IFN-γ was efficiently produced after longer incubation, showing that the short pulse of NKT cells with plate-bound αGC-CD1d complexes could recapitulate the OCH phenotype. These results demonstrate that the timing of the CD1d-lipid interaction rather than the "shape" of the OCH-CD1d complex is the decisive factor in controlling polarization of cytokine production by NKT cells.

Differential transcriptional properties of cytokine genes. To clarify the molecular basis for different kinetics of cytokine production by activated NKT cells, we next examined the effects of CsA or CHX on the NKT cell responses. Without any inhibitors, IL-4 production was more rapid and had a higher rate than IFN-γ production (Figure 3C), confirming the kinetic difference required for induction of each cytokine shown in Figure 3A. Production of both IL-4

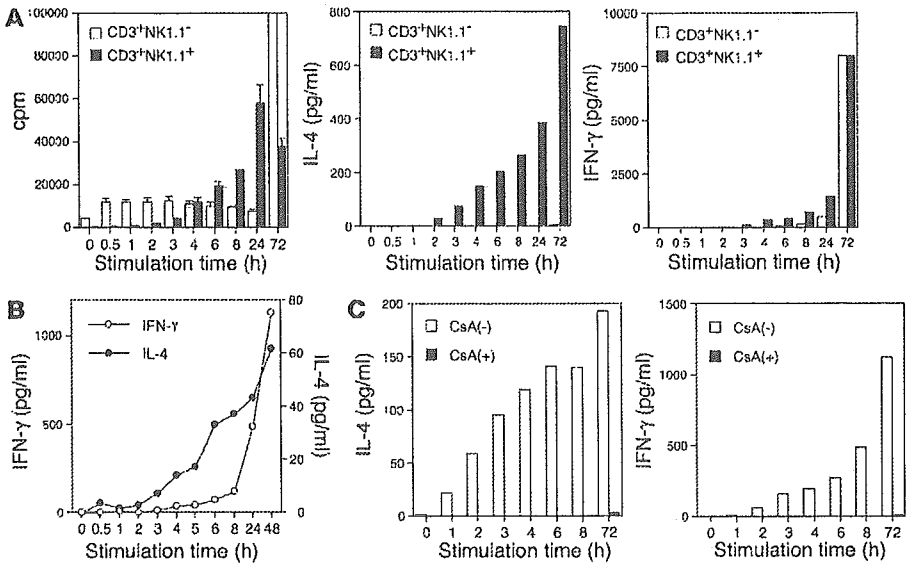

Figure 3

Kinetic analysis of NKT cell activation and cytokine production after glycolipid stimulation. (**A**) Differential production of IFN-γ and IL-4 by activated NKT cells. CD3+NK1.1+ NKT cells and conventional CD3+NK1.1− T cells were purified from liver mononuclear cells by cell sorting. The sorted cells were stimulated with immobilized mAb to CD3 for the time indicated on the *x* axis and were then removed and recultured on a fresh culture plate without anti-CD3 stimulation for up to 72 hours from the start of the anti-CD3 stimulation. Incorporation of [^{3}H]thymidine (1 μCi/well) during the final 16 hours of the culture was assessed (left), and culture supernatants were analyzed for the production of IL-4 (center) and IFN-γ (right) by ELISA. One experiment representative of three independent experiments with similar results is shown. (**B**) NKT cells purified from liver mononuclear cells were stimulated with plates coated with DimerX I loaded with αGC and were analyzed as shown in **A**. (**C**) NKT cells purified from liver mononuclear cells were stimulated as shown in **A** in the presence [CsA(+)] or absence [CsA(−)] of CsA (1 μg/ml). Culture supernatants were analyzed for the production of IL-4 and IFN-γ by ELISA.

and IFN-γ after TCR stimulation, however, was almost completely inhibited by pretreatment of NKT cells with CsA.

Similarly, CsA abolished the transcriptional activation of *IL-4* and *IFN-γ* genes in activated NKT cells (Figure 4A), indicating that TCR signal–induced activation of nuclear factor of activated T cell (NF-AT) is indispensable for the production of both cytokines by NKT cells. Meanwhile, transcription of these cytokine genes showed different sensitivities to CHX treatment (Figure 4A). Although transcriptional activation of *IL-4* was barely affected by CHX treatment, transcription of *IFN-γ* gene was almost completely blocked after treatment with CHX. These results indicate that transcriptional activation of *IFN-γ*, but not that of *IL-4*, requires de novo protein synthesis.

Next, we analyzed the sensitivities of other cytokine genes to CsA and CHX treatment (15–17). As shown in Figure 4B, transcriptional activation of all cytokine genes tested was completely blocked by pretreatment of NKT cells with CsA. Interestingly, transcription of the *IL-2* gene and *GM-CSF* gene were blocked by CHX treatment. In contrast, transcriptional activation of *TNF-α* was resistant to CHX treatment. These results indicate that cytokines produced by NKT cells could be divided into two groups based on their dependence on de novo protein synthesis.

Selective c-Rel induction after stimulation with αGC. Although NKT cells secrete a large number of cytokines upon stimulation, the regulatory mechanisms for the expression of each cytokine are still poorly understood. The susceptibility of IFN-γ production to CHX indicates that some newly synthesized protein(s) would promote specific transcription of the *IFN-γ* gene in NKT cells. To identify the protein responsible for αGC-induced transcription of the *IFN-γ* gene, we purified NKT cells from glycolipid-administered I-A^{b}β–deficient mice, which have two- to threefold higher numbers of NKT cells in the liver and the spleen than do wild-type B6 mice (18), and assessed NKT cell–derived total RNA by microarray analysis. As shown in Table 2, a number of cytokines and chemokines were differentially expressed after in vivo treatment with either αGC or OCH. It is noteworthy, however, that significant induction of *IFN-γ* transcription was observed only in αGC-treated samples, not in OCH-treated samples. Overall, the data obtained correlated well with previous results showing that OCH is a selective inducer of IL-4 production from NKT cells (9). There was no transcriptional upregulation of cytokines genes such as the *IFN-γ* and *IL-4* genes 12 hours after treatment with either glycolipid, indicating that NKT cells have undergone quiescence at this time point in the context of transcriptional upregulation of cytokine genes, although some genes are still upregulated.

Through analyzing the microarray data, we identified the protooncogene *c-Rel*, a member of the NF-κB family of transcription factors, as a candidate molecule that may play a role in the *IFN-γ* transcription. As shown in Figure 5A, *c-Rel* was inducibly expressed in NKT cells 1.5 hours after stimulation with αGC. In contrast, OCH treatment did not induce *c-Rel* transcription (Figure 5A). The transcription of other NF-κB family genes such as *p65/RelA* and *RelB* was not upregulated after treatment with αGC or OCH. Real-time PCR analysis also confirmed the selective induction of *c-Rel* after αGC stimulation (Figure 5B). CsA treatment inhibited *c-Rel* transcription, but CHX did not (Figure 5C), indicating that the inducible transcription of c-Rel is directly controlled by TCR signal–mediated activation of the NF-AT (19).

It is already known that c-Rel serves as a pivotal transcription factor for the Th1 response that would directly induce IFN-γ production in conventional T cells (20). However, very little is known about the function of this protooncogene in NKT cells during TCR-mediated activation. We therefore conducted time course analysis for transcriptional activation of *c-Rel* in parallel with *IL-4* and *IFN-γ*. We stimulated NKT cells with immobilized mAb to CD3 for 30–100 minutes and then cultured them without further stimulation for a total of 120 minutes. As shown in Figure 5D, *IFN-γ* expression was slightly downregulated in the first 90 minutes of TCR stimulation and was significantly upregulated when the cells were stimulated for 100 minutes. Interestingly, we found that the kinetics of *c-Rel* transcription were similar to those of *IFN-γ* transcription (Figure 5D, right). In contrast, transcrip-